

**REDUCTION OF RESERVE MARGIN WITH INCREASING WIND
PENETRATION: A QUANTITATIVE FIRST-PRINCIPLES ANALYSIS**

by

Josiah Caleb McClurg

A thesis submitted in partial fulfillment
of the requirements for the Master of
Science degree in Electrical and Computer Engineering
in the Graduate College of
the University of Iowa

July 2012

Thesis Supervisor: Assistant Professor Raghuraman Mudumbai

Copyright by
JOSIAH CALEB MCCLURG
2012
All Rights Reserved

To my brother, sisters, and parents.

A Wind that rose though not a Leaf
In any Forest stirred,
But with itself did cold engage
Beyond the Realm of Bird.
A Wind that woke a lone Delight
Like Separation's Swell –
Restored in Arctic Confidence
To the Invisible.

– Emily Dickinson

ACKNOWLEDGEMENTS

I would like to acknowledge my advisors, my professors, and the many fellow students who continue to challenge and inspire me.

ABSTRACT

Access to reliable electric power is considered by the developed world to be a minimum requirement for a reasonable standard of living. In addition to meeting a fluctuating demand, the modern electricity industry must now integrate intermittent generation sources like wind into the grid. Reserve margin allocation (RMA) for an acceptable loss of load expectation (LOLE) allows traditional generators to maintain grid reliability in the presence of small penetrations of wind energy. However, traditional RMA over-allocates the reserve capacity in the presence of short-term intermittency mitigation techniques like energy storage and demand response. For economic operation of the modern, grid better characterization techniques are needed for reserve margin reduction behavior in the presence of wind energy. This thesis addresses this challenge with a quantitative RMA analysis using real-world and simulated wind data for three different grid scenarios, with and without intermittency mitigation. The research is novel in its first-principles approach and its investigation into the practical validity of the analogy between demand response and energy response.

TABLE OF CONTENTS

LIST OF TABLES	viii
LIST OF FIGURES	ix
CHAPTER	
1. INTRODUCTION	1
Background Synopsis	1
Related Work	3
Contributions	4
Organization of Thesis	5
2. BACKGROUND AND MOTIVATION	7
Lessons from History	7
Energy as basic research	8
Industrial product development	9
Politicians Invest in Science	10
Economic Collapse and Social Influences	11
What we've learned	12
Grid Operations	14
Response to Variable Load	14
Response to Intermittent Generation	16
3. OUR CONTRIBUTION	18
Methods	18
Theoretical Motivation	18
Relationship between reserve margin and mean wind power	18
Relationship between storage, demand response, and reserve margin.	23
Hypotheses	24
Data Collection and Preprocessing	27
Data Sources	27
Preprocessing Flow	27
Descriptions and Discussion of Individual Datasets	31
Simulation Architecture	44
Idealized Energy Storage Device	46
Idealized Demand Response	48
Results	48
Effects of high wind penetrations on RMA	50
Reserve Margin Calculations	50
Auto- and Cross-Correlations	54
Effects of energy storage and demand response on RMA	61
Demand Response	65
Energy Storage	65
4. CONCLUSION AND FUTURE RESEARCH	72
Data Preprocessing and Wind Simulation	72

Reserve Margin Characteristics	72
Intermittency Mitigation Behavior	73
BIBLIOGRAPHY	76

LIST OF TABLES

Table 1. List of hypotheses.....	5
Table 2. List of hypotheses.....	24
Table 3. Table of real-world information sources	25
Table 4. Table of simulated wind power sources.....	26
Table 5. Summary of raw dataset parameters	30
Table 6. Haina wind gap information.....	35
Table 7. Chosen turbine parameters for converting the Haina wind speed to power.....	37
Table 8. Turbine parameters for Vestas turbines, 2MW or less.....	37
Table 9. List of hypotheses.....	49
Table 10. Reserve margin reduction performance ordering of real wind power.....	55
Table 11. Reserve margin reduction performance ordering of simulated wind power	55
Table 12. Absolute sums of cross correlation functions.....	56
Table 13. Predicted performance rank of load based on autocorrelation compared to observed rank	59
Table 14. Predicted performance rank of real wind power based on autocorrelation compared to observed rank.....	59

LIST OF FIGURES

Figure 1. Organization of thesis and primary results	6
Figure 2. Timeline of electrical innovations	8
Figure 3. Formation of the modern grid.....	13
Figure 4. Responding to load variations on different time scales	15
Figure 5. Relating reserve margin to wind and load statistics.....	20
Figure 6. Taylor series approximation of cumulative distribution function.....	21
Figure 7. Illustration of demand response and energy storage.....	23
Figure 8. Preprocessing flow for real-world and simulated datasets	28
Figure 9. Detrending procedure.....	29
Figure 10. Wind farm power extraction curves for three example sites corresponding to high (Class I), medium (Class II) and low (Class III) wind speeds.....	31
Figure 11. “Box plot” of power and speed in the frequency domain, showing the minimum and maximum spectral components, along with the mean, 1 st and 3 rd quartiles.....	32
Figure 12. “Goodness of fit” analysis, demonstrating that the datasets followed a Weibull distribution in their long-term characteristics.	33
Figure 13. Long term probability map of site data. The y axis represents the site characteristic (mean wind speed or power), the x axis represents observed wind speed or power.	34
Figure 14. Differences between the autocorrelation functions of the no-gap data, with the gap-adjusted and non-adjusted data	36
Figure 15. Differences between the spectral velocity of the no-gap data, with the gap-adjusted and non-adjusted data.	36
Figure 16. Detrending process for MISO load.....	38
Figure 17. Detrending process for MISO wind.....	38
Figure 18. Process for Filtered Gaussian Model	41
Figure 19. Illustration of filtering process.....	41
Figure 20. Load profile showing the effects of filtering spectral peaks.....	42
Figure 21. Wind profile showing effects of filtering spectral peaks.....	43

Figure 22. Simulation model overview	45
Figure 23. Algorithm for energy storage model.....	46
Figure 24. Algorithm for demand response model.....	47
Figure 25. Reserve margin calculations for real-world wind generation data	51
Figure 26. Reserve margin calculations for simulated wind data	52
Figure 27. Marginal reserve variation with respect to degree of aggregation and wind penetration.....	53
Figure 28. Histograms of marginal reserve requirements for individual sites of the NREL dataset.....	54
Figure 29. Cross correlations of real-world wind power with the various loads	57
Figure 30. Cross-correlations of simulated wind power with the various loads	58
Figure 31. Wind power autocorrelation plots, detailing the lags at which the autocorrelation reaches 20% and 0% of maximum.	60
Figure 32. Autocorrelation of loads, detailing location of first large correlation trough.	61
Figure 33. Power spectra of real wind.....	62
Figure 34. Power Spectra of loads.....	63
Figure 35. Power spectra of simulated wind	64
Figure 36. Reserve margin reductions from base-case under “mid term” demand response (up to 50 hours).....	66
Figure 37. Reserve margin reductions from base-case under “long term” demand response (up to 200 hours).....	67
Figure 38. Reserve margin reductions, in extreme case demand response (up to 800 hours)	68
Figure 39. Mid-capacity (up to 500 hours mean wind).....	69
Figure 40. Large capacity (up to 2000 hours of mean wind)	70
Figure 41. Extreme-case energy storage capacity (up to 8000 hours of mean wind)	71

CHAPTER 1

INTRODUCTION

This thesis is organized into four chapters. This initial chapter provides a brief synopsis of the background material and summarizes our primary results in light of the previous reserve margin allocation research. Chapter two is designed to provide background material and “big picture” motivation for the study. The second chapter begins by outlining the development of the electric grid and concludes with an overview of modern electric generation. Chapter three represents the heart of this thesis – a two-part statistical reserve margin allocation analysis of real world wind power and grid load data. The first section of chapter three addresses the theoretical motivation for our investigation, dataset considerations, and simulation architecture. The second section of chapter three examines the quantitative results of high wind penetrations and intermittency mitigation technologies on reserve margin allocation. The final chapter in this thesis presents a summary of the conclusions of chapter three, along with suggestions for future research.

Background Synopsis

The tumultuous 133-year history of the commercial electric grid in the United States provides significant evidence to support the following three suppositions about large-scale grid dynamics:

1. Competition drives the development of new grid-related technologies.
2. Public policy determines which new technologies are integrated into the grid.
3. Operation economics determine whether or not a new technology is here to stay.

If the electric power industry is to remain healthy, engineers must optimize the competitive framework, public policy implications, and economics of the grid. One of the primary ways in which this complex three-way optimization is being addressed is through

the large-scale integration of wind generation into the electric grid. The distributed nature of wind farms tends to support a more “open” grid, which encourages competition among electricity providers. U.S. public policy has been very supportive of wind energy since the late 1970’s, and more recently has disbursed substantial wind energy funding with the EPACT of 2005 and the more recent Recovery Act of 2009. Moreover, the lifecycle economics of wind energy are currently significantly more mature than other industry-ready sustainable technologies [1].

One of the supporting factors for the widespread integration of wind energy into the existing grid is that the current grid is already designed to support periodic variations in load. A technique called frequency control mode allows generators to adjust to small changes in load in a matter of seconds. And, for larger unexpected load variations, grid operators have access to high ramp-rate “peaker” plants capable of reaching full output capacity in minutes and can purchase power on demand if necessary from other independent electric grids via grid interconnects. Today, reliability is guaranteed by over-provisioning generation capacity some 1% above peak historical load (assuming worst-case wind generation output) such that the LOLE (loss of load expectation) is less than 0.027% (1 day in 10 years) [2]. The determination of the necessary generation capacity to meet the required LOLE is known as Reserve Margin Allocation (RMA). Despite all of the measures that are in place to ensure the grid’s robustness, excessive unpredictable variation can be extremely costly and therefore should be avoided if possible.

Wind penetration is defined as the ratio of wind generation to the total load. At low penetrations of wind generation, the intermittency in generation caused by wind can simply be viewed as additional “noise” on top of the demand curve. However, as the penetration of wind increases, the variability in generation becomes too great for traditional grid technologies to accommodate economically. The stiff penalties for “dropping” a unit of required load, and the expense of frequently operating “peaker” plants far overshadow the aggregate decrease in traditional generation requirements.

Thus, under high penetrations of wind, short-term intermittency mitigation technologies such as energy storage and demand response (DR) are needed to reduce the variability of aggregate wind generation output to a level at which the economics and politics of running a reliable grid make sense [3]. This competitive new field of intermittency mitigation technology has already fostered substantial innovation, and promises much more for the future.

Yet, despite substantial advances in the implementation technology for energy storage and demand response, there remains a growing need for high-level integrated assessment models to aid in the planning and policymaking related to wind energy [4]. This thesis investigates the fundamental constraints and modeling considerations of reserve margin allocation at high wind penetrations and discusses the quantitative effects of energy storage, and demand response on reserve margin reduction.

Related Work

Our work differs from previous research in two ways. First, it is a first-principles analysis which avoids market considerations in preference for engineering solutions. Previous scholarly work related to the effects of high wind penetrations on RMA have focused primarily on the costs associated with intermittency [5], and utilize complex industry models to predict market behavior [6]. In this thesis, we have specifically avoided the use of such market-based methods, to favor a more first-principles RMA approach. The benefit of this method is the freedom to gain insight into the fundamental physical limits of reliable wind generation without the tight practical constraints associated with the reserve margin calculations undertaken each year by the major electricity suppliers. Our initial results yield intuition into the statistical characteristics of wind which are important to long term allocation planning, and include a comparison of four different wind simulation models.

The second way in which our work differs from previous research is that it provides a quantitative comparison between demand response and energy storage, rather than assuming the analogy a priori as in [7]. Substantial previous research has been accomplished in the fields of energy storage sizing for wind applications [8], and a number of studies have assessed demand response potential [9]. This thesis, however, specifically compares the ability of ideal demand response and energy storage models to reduce the reserve margin under high wind penetrations. First, we establish that large capacities of energy storage and large maximum delays of demand response are required for significant reserve margin reduction. Second, our initial results indicate that the relationship between demand response and energy storage is decidedly distinct from the straightforward “virtual storage” or “capacity credit” concepts often used when discussing the benefit of demand response.

Contributions

This thesis presents a first-principles RMA analysis for three different real-world grid scenarios corresponding to large, medium, and small independent grids under high wind penetration and in the presence of energy storage and demand response. The reserve margin behavior at a range of wind penetrations is calculated for seven different real-world and simulated wind power scenarios ranging in scope from a centralized model to an large-scale distributed wind power profile. This thesis further develops these results by considering the effect of adding energy storage and demand response to each of these scenarios at 1%, 10%, and 100% wind penetration. In addition to contributing a statistical framework, software tools, and an evaluation of dataset considerations, this thesis applies its quantitative results to address the six important hypotheses listed in Table 1. These hypotheses are motivated by theoretical results of our statistical framework.

Initial Hypothesis	Result
1. Reserve margin reductions are close to the mean wind at low wind penetrations	True
2. Degree of reserve margin reductions will decrease with increasing wind penetration	True
3. High correlation of wind power with itself and with load both have a negative impact on reserve margin reduction	True
4. Geographic distribution of wind turbines result in a reduction of correlation and therefore increased suitability for reserve margin reduction	True
5. Benefits of demand response and energy storage are minimal at low deployment	True
6. Energy storage capacity of T hours of mean wind power is roughly equivalent to demand response delay limit of T hours.	False

Table 1. List of hypotheses

Organization of Thesis

Figure 1 graphically illustrates the organization of the rest of this thesis, and should be read top to bottom, left to right. The arrows illustrate the dependency relationships, or “motivation hierarchy” of our primary results. Chapter two supplies a brief history of the electric grid and a description of current grid operations in order to provide the long-term perspective and the immediate industry context in which to view our contribution. Chapter three describes the methods and results of our research. The methods section contains a theoretical discussion which motivates a list of hypotheses to be examined; a detailed description of the individual data sources used and discussions of the effects of preprocessing; and a presentation of a new wind power model along with an outline of the simulation software architecture. The results section of the third chapter presents graphs, tables, and discussions relating to the hypotheses presented in the methods section. Finally, chapter four offers a summary of our results and comments on future work related to this thesis.

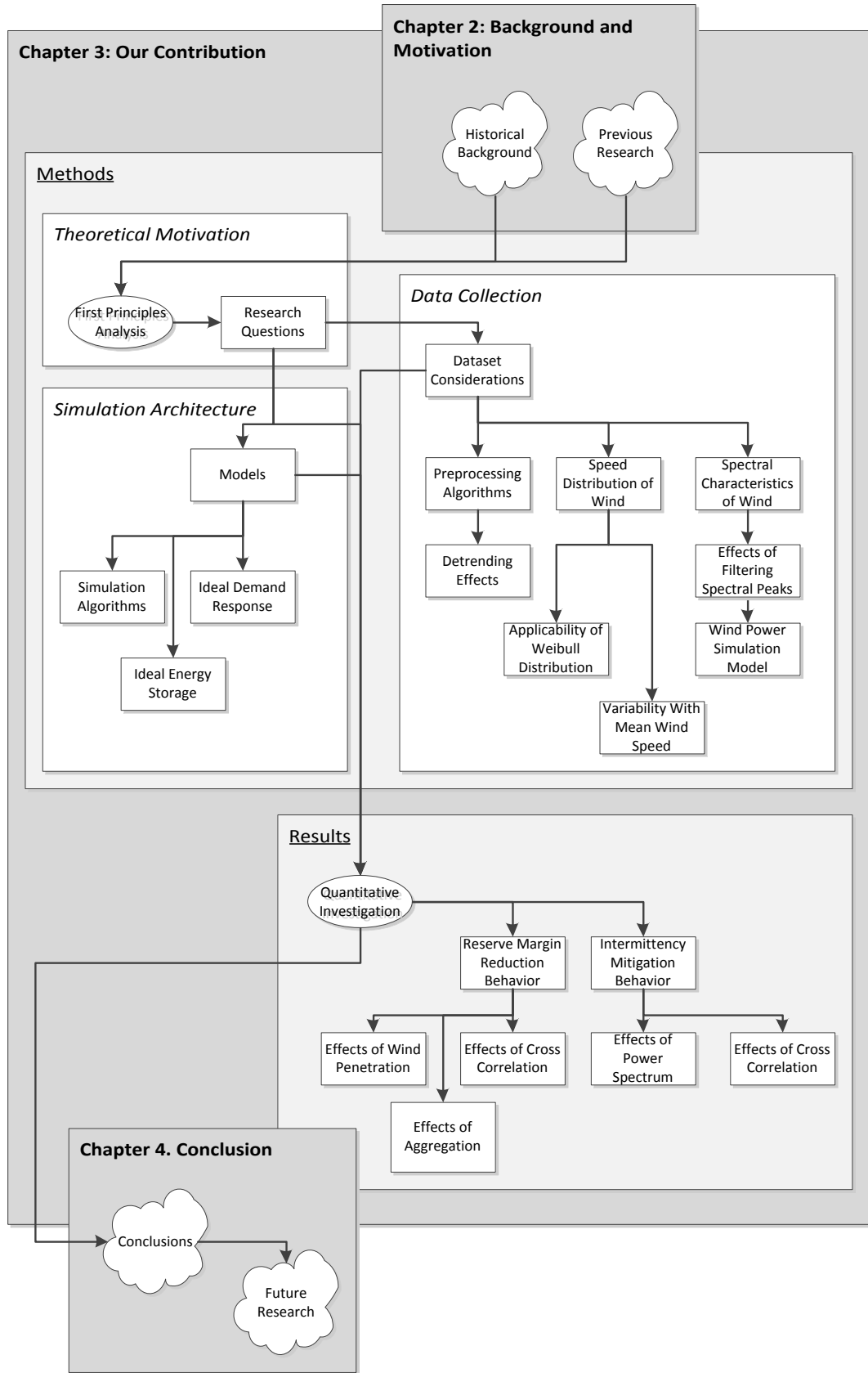


Figure 1. Organization of thesis and primary results

CHAPTER 2

BACKGROUND AND MOTIVATION

Lessons from History

The problem of mitigating intermittent grid conditions is not a new one. Electrical operators have been responding to fluctuating loads since Edison's time – well over a century ago. However, the industrial, political, and social climate of today offers power operators a distinctly different set of technical and non-technical challenges than those they have faced in the past. To augment the quantitative results of our study and the technical implications of our statistical framework, it is helpful to obtain a grasp of the complex social, political, and economic factors that have influenced the development of the electrical grid throughout history.

Electricity has become so commonplace that it is easy to forget the sheer wonder of living in a world where ubiquitous on-demand access to unlimited electrical power is to be had for pennies per kilowatt-hour. The steps humanity has taken to attain this astounding technical achievement were not easy. Like other stories of grand scope and sway, the history of the electrical grid is riddled with tales of intrigue, exhilaration, greed, corruption, genius, heartbreak, and friendship. However, unlike many other historical narratives which weave their tale circuitously and gradually, the story of the grid is decidedly disjoint – punctuated neatly by three transformative events: The commercially-viable electric light bulb (which transformed electricity from a scientific curiosity to a commercial product); the atom bomb (which resulted in a nuclear energy program which nearly bankrupted the electric power industry); and the oil embargo of 1973 (which introduced the political and social motivation for a move toward privatization and environmentally conscious electricity generation).

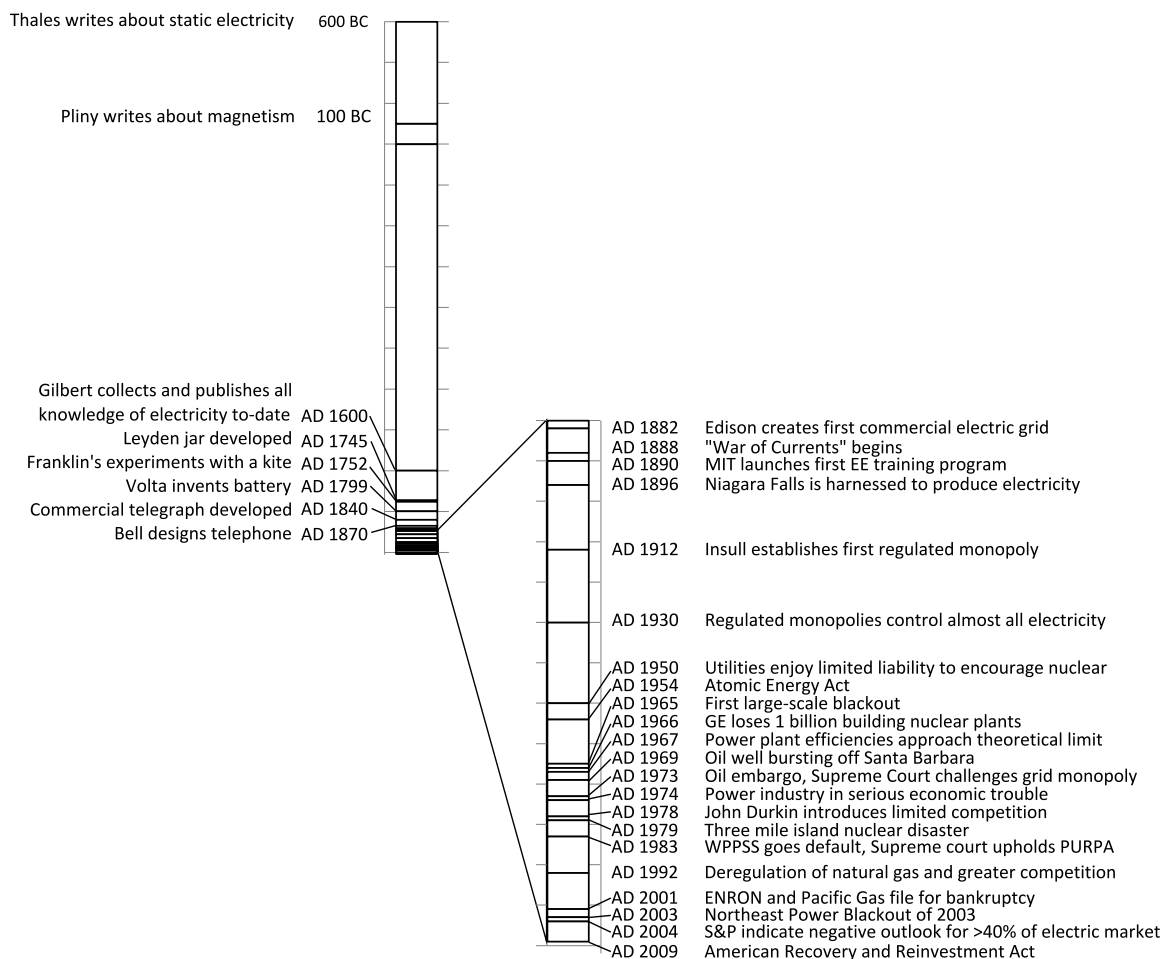


Figure 2. Timeline of electrical innovations (highlights from [10] and [11])

Energy as basic research

Thales of Miletus' descriptions of the behavior of amber, rubber, and lodestones from 600 B.C. are the first recorded deductive observations of the basic electromagnetic laws that govern the operation of all electrically-powered devices today. However, Thales' primary interest in electricity was not to understand its physical behavior. Instead, he studied the phenomenon in order to support a particular metaphysical philosophy. Thus, aside from its reverent awe of lightning, humanity did not seriously investigate electrical phenomena again for almost a millennium. In A.D. 1600, a century after Europe's Dark Ages, an astronomer named William Gilbert published a single

volume which contained the whole of human knowledge about electricity and magnetism to-date. This volume sparked interest among scholars across Europe and people began investigate the phenomenon further.

In 1650, Otto von Guericke developed a simple electrostatic generator. Some years later, in 1747, Musschenbroek developed a basic capacitor, which became the first example of electrical storage. This device was spectacularly demonstrated to the king of France by Benjamin Franklin's gravest scientific opponent, Jean Nollet: After instructing seven hundred friars to hold hands and form a circle, Nollet reputedly discharged enough power through this monkish circuit to cause them all to simultaneously leap into the air.

In the years that followed, Franklin, Ohm, Kirchhoff, Ampere, Faraday, Maxwell and others made significant contributions to electrical theory. However, even seemingly revolutionary technologies like the battery and the electric motor were little more than scientific curiosities at the time of their invention. In fact, Hungarian scientist Anyos Jedlik, the inventor of the electric generator, did not even apply to patent his device. While the vast majority of contributions during this period were purely scientific in nature, Volta's battery did prove sufficient to support a handful of commercial technologies like the telegraph in 1840, as well as the telephone in 1870.

Industrial product development

Apart from the telegraph and telephone, electricity remained a scientific curiosity and was largely distinct from commerce. The scientific community had taken an important step in working out the theory of how to generate, control, transmit, and store electricity. However there simply was not sufficient widespread demand for this new form of energy to merit a large-scale generation and distribution system for electricity. To consumers of the day, the modern energy needs seemed to be already more than met. Gas made it possible for people to cook their food, obtain hot water, and turn on the lights – all with only the turn of a valve. The coal-fired steam engine powered great factories and

a burgeoning railway system that spanned the nation. In fact, the first commercially-viable electrical technology that required any substantial amount of power encountered strong opposition from many sectors. When Edison introduced his electric light bulb to the world, it took substantial market intervention, immense litigation, and no small amount of bribery to create the demand and infrastructure needed to support the first electric grid.

The famous “war of currents” between Edison and Westinghouse (allied with the genius inventor Nikola Tesla, who had left Edison’s employ due to poor wages) is a well-documented [12] and intriguing tale in itself. In summary, alternating current prevailed due to the lack of an efficient DC equivalent of the voltage transformer. Because the transformer made it possible for large volumes of power to be efficiently transported long distance, the electric grid began to develop around a centralized generation model. After leaving General Electric, Samuel Insul, Edison’s former private secretary, later became a key player in the utility industry. He successfully pushed for widespread government regulation of utilities in order to avoid the hassle dealing with individual municipalities. Technology and science continued to improve through scholarly journals like the transactions of the AEE (now IEEE), founded just four years after Edison implemented his light bulb. Electrical research during this era was primarily motivated by market factors of the utility industry, and the field experienced incremental rather than transformative changes.

Politicians Invest in Science

By 1930, almost all electricity generated in the united states was controlled by regulated utilities. In fact, the largest monopoly at this time controlled 40% [10] of the nations electric power. Moreover, New Deal legislation during the Great Depression of the late 1930s opened the door for Federal control of these public utilities, moving electricity regulation from the regional to the national level.

By the end of World War II, the U.S. economy was booming. After the war, the U.S. government was eager to harness the power of the atom to generate inexpensive energy and began to fund industrial research toward that goal. The 1950s brought about limited liability legislation, which freed utilities from some of the financial risks associated with building and operating a nuclear plant, and the Atomic Energy act of 1954 added further financial incentives for utilities to develop a nuclear power infrastructure.

Despite these incentives, the U.S. power industry remained reluctant to integrate nuclear power into their existing generation and distribution systems. The late 1950s and early 1960s were a period of financial and technical difficulties for electric utilities. This was exemplified by the large scale blackout occurring in 1965, and GE's reported \$1 billion loss in income in 1966 due to unexpected costs of nuclear power integration. In 1967, conventional power plants had reached the practical (and nearly the theoretical) limit for efficiency, and therefore ceased to become cheaper to build and operate. Generation costs had increased, demand continued to rise, and yet prices remained fixed by law. The industry entered serious economic turmoil.

Economic Collapse and Social Influences

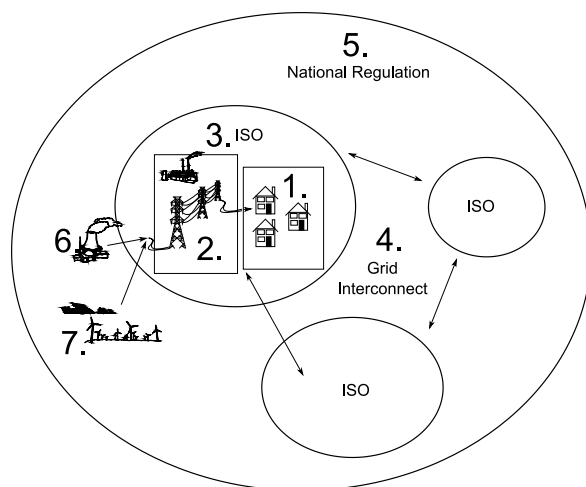
The bursting of an oil well off the coast of Santa Barbara, California in 1969 incited environmentalist groups to question the long term effects of fossil fuels. However, it took the economic difficulties brought on by the oil embargo of 1973 to catalyze changes in public policy. The next year, the National Renewable Energy Laboratory (NREL) was founded to support renewable energy alternatives to traditional generation. In an attempt to boost the economy and lessen dependence on foreign oil, the power of the utility monopolies was challenged and private utilities were slowly given more autonomy. As a result of senator John Durkin, utilities were allowed to exercise a limited form of market competition in 1978. And, while the nuclear plants were not living up to

their predictions of producing “electricity too cheap to meter,” the lavish investment in nuclear power of the decade before seemed to be slowly paying off.

And then came the Three-Mile Island nuclear disaster of 1979. The insurance, regulatory, and safety costs associated with building a new nuclear plant skyrocketed. The production of new nuclear plants was abruptly halted just at a time when the electricity industry was in dire need of an economical and reliable way to generate power. In 1983, WPPSS, a major electric power utility went bankrupt. The same year, the Supreme Court upheld regulation to allow federal intervention to increase efficiency of generation. Despite the Energy Policy Act of 1992, which opened the door to greater competition among public utilities, the industry continued to experience financial difficulties. The ENRON scandal and subsequent bankruptcy filing of Pacific Gas and Electric in 2001 only added to the downward spiral of the industry. In 2004, Standard and Poor indicated a negative outlook for more than 40% of the electricity market [10]. In an attempt to get the industry back on its feet, Congress passed bills in 2005, 2007, and most recently 2009 that dedicated substantial funds to renewable energy research and smart grid. Despite these efforts, 2010 saw corporate research and development in renewable energy decrease significantly [13] – largely for financial reasons.

What we’ve learned

Figure 3 illustrates the historical progression of the technology and political structures that make up the current electrical grid. Today, there are three primary influences that are changing the “big picture” of how the electric grid works: competition, political and public policy factors, and market economics. The war of currents showed the innovation brought on by competition, and Samuel Insul demonstrated practical benefits from regulated monopolies. The stability of monopolies combined with continual incremental technology improvements of the late 1800s and early 1900s allowed the electric power industry to gain the reputation of “keeping the lights on, for cheap” among



1. Edison creates demand for electricity and first practical distribution system.
2. Westinghouse successfully pushes for centralized generation model (long distance transmission lines)
3. Samuel Insul successfully pushes for regulated utilities to limit competition and cut down operating expenses of running thousands of power plants.
4. Market economics dictates sale of electricity between large companies
5. National scale regulation under New Deal
6. Strong political push to develop nuclear energy, increased regulation.
7. Renewable technologies begin to be integrated after oil embargo

Figure 3. Formation of the modern grid

consumers, while providing a stable source of profitable income to utility investors. Since then, economic profitability of the electric power industry has slowed. There are heavy penalties for not meeting power demand, and the environmental regulations following the oil embargo have added additional costs to the power industry's already-tight budget. Despite the recent government investments in renewable energy research, technological progress in the industry is erratic and many investors have lost faith in the financial stability of electric utilities.

Government assistance continues to mitigate the economic difficulties of utilities and to fund important sustainable energy research – however, if the electric power industry is to continue, it must restore the faith of investors. Whether that means a return to the “slow and steady” profits of ages past, or a transformative entry into the exciting cutting-edge technology sector, utilities must integrate high penetrations of sustainable energy. To do this, the problem of intermittent generation must be addressed. Importantly, sustainable generation must be made profitable if it is to survive beyond the

current government subsidy. For intermittent generation to become profitable, it must be based on sound engineering and tested principles rather relying solely on market mechanisms. It is with this kind of first-principles engineering analysis that this thesis proceeds. In particular, this thesis addresses the problem of reserve margin allocation to ensure the reliability of the grid despite the presence of a significant degree of intermittent wind generation and investigates the ability of energy storage and demand response to reduce the reserve requirements.

Grid Operations

Response to Variable Load

Even without any intermittent generation, the electric grid experiences significant variation in load over the course of time, and must respond to these changes. Because most of the variation is predictable, the majority of generation is scheduled ahead of time. Traditionally, the primary difficulty with this scheduling has been to minimize the costs to the generating utility. This cost minimization primarily occurs at the three different time scales illustrated by Figure 4.

Cost minimization over long time periods (days) is mostly related to the problem of determining when to fire up and when to power down a particular power plant. This procedure is known as unit commitment. A shorter time-scale problem (hours), known as economic dispatch, involves allocating generation optimally among those power plants which are currently running. The same problem, reduced to the scale of allocating individual generators within a power plant is known as secondary control and has a time frame of minutes. Because the demand at each of these time scales is essentially known, optimal control methods can be used at each one of these different time scales to ensure lowest cost generation.

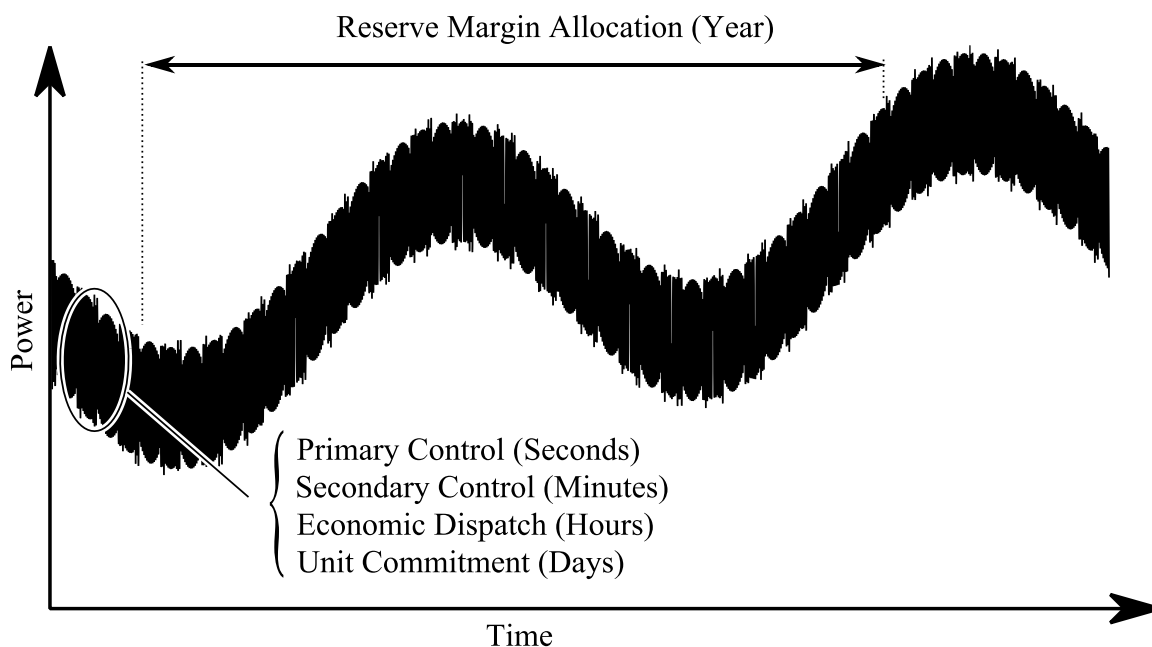


Figure 4. Responding to load variations on different time scales

During normal grid operation (i.e. no faults), it is only at the shortest time scale (seconds) that traditional generators must deal with a significant degree of uncertainty. Since the earliest days of the grid, a method known as frequency control mode has been used to allow generators to sense whether to increase or decrease their power output in response to changes in load. Several times a second, the generator control system makes a measurement of the grid frequency. If the grid frequency is above nominal, the generator reduces its power output to compensate for the reduced load. If the frequency is below nominal, the generator increases its power output to adjust for an increased load. Given a large enough spinning reserve and sufficient transmission capacity, the frequency control mode can account for most fluctuations in load.

However, to account for unexpected long-term increases in demand (an unexpectedly hot day, for instance), the electricity provider also operates a number of fast ramp-rate “peaker” plants. In order to start up quickly, these plants typically burn natural gas and potentially petroleum and run at much lower efficiencies than base-load plants.

Because of the reduced efficiency, “peaker” plants are much more expensive to operate than base-load plants.

An annual review of the unexpected variations in load allows grid operators to improve their predictions and to plan for building new generation capacity. In order to avoid the significant costs associated with failing to service a load (known as a dropped load), electric utilities complete what is known as reserve margin allocation (RMA) to ensure a certain minimum probability of outage. This probability is called the LOLE, or loss of load expectation. Reserve margin planning is similar to the previously-discussed scheduling problems in that it involves an allocation of power. However, it is different in that RMA allocates for worst case demand, while the shorter time scale generation scheduling methods allocate for most likely demand.

Response to Intermittent Generation

While wind power at low penetrations can be considered simply as additional variability of the demand, larger wind penetrations introduce too much variability for the electric grid to economically accommodate [1]. There are two primary methods of removing this variability. The act of removing the variability of an intermittent generation source is known as intermittency mitigation.

The first intermittency mitigation technique is to add energy storage to “smooth” the power output of intermittent generators. Energy storage covers a wide variety of technologies, ranging from batteries and capacitors, to pumped fluids and biomass. These technologies also cover a wide range of time scales as well, with full-power duration of storage ranging from a couple of seconds up to four months [14]. Batteries, by far are the most commonly-investigated storage option, due to their competitive cost and comparatively fast charge and discharge rates [8]. This thesis considers a battery-like energy storage model.

The second method of intermittency mitigation is known as demand response. The idea behind demand response is to adjust demand to match the available supply. Consumers can adjust their demand in three ways. First, consumers may shift electricity usage to off-peak hours. Second consumers can reduce electricity usage during peak hours. Third, some consumers can meet some of their electricity requirements with on-site generation [15]. To encourage participation in demand response programs, electricity companies offer monetary incentives and manipulate electricity prices. These two motivation techniques are known, respectively, as incentive-based programs and price-based programs [9]. In this thesis, we do not investigate market factors such as pricing but instead consider an idealized a demand response model based on load shifting.

To further a better fundamental understanding of wind energy and intermittency mitigation on reserve margin, this thesis performs a first-principles RMA on a number of real-world wind and load datasets. In particular, we assess the reserve margin effects of increasing wind penetration and the incorporation of intermittency mitigation techniques. The following chapter discusses this contribution in detail.

CHAPTER 3

OUR CONTRIBUTION

This chapter presents the methods and primary results of our contribution. The methods section provides a theoretical motivation which develops six research questions for investigation, a description of the data sources used which details preprocessing considerations, and an outline of the simulation architecture. The results section contains the results of our simulations and discusses how these results relate to the research questions posed in Table 2.

Methods

Theoretical Motivation

The theoretical motivation for this thesis is a first principles statistical analysis that results in six research questions related to the properties of reserve margin under increasing wind penetration, used in conjunction with energy storage and demand response technologies.

Relationship between reserve margin and mean wind power

Because reserve margin is a practical engineering expression rather than a mathematical term, it may be calculated in a wide variety of ways [16]. In this thesis, we define the reserve margin to be the minimum constant generation capacity value M which satisfies a given loss of load probability (LOLP) constraint. That is, given that L and W are positive random processes representing the grid load and the generated wind power respectively, reserve margin is the M which guarantees a sufficiently small probability of outage:

$$\Pr(W + M \leq L) \leq \text{LOLP}$$

Now, assuming W and L are jointly stationary and ergodic, the probability density function of the grid load L is given by $f_L(x) \equiv \lim_{\varepsilon \rightarrow 0} \Pr(x \leq L \leq x + \varepsilon)$. For convenience, let us use the notation $f_L(x) = \Pr(L \rightarrow x)$. Next, define $F_W(x) \equiv \Pr(W \leq x)$ to be the cumulative distribution function of the wind power. Re-arranging and integrating over all values of x , we obtain:

$$\Pr(W \leq L - M) \leq \text{LOLP}$$

$$\Pr(W \leq L - M) \equiv \int_{-\infty}^{\infty} \Pr(L \rightarrow x \text{ and } (W \leq \ell - M)|_{\ell=x}) dx$$

If we assume a maximum wind generation capacity $MaxWind$ and furthermore assume that L and W are stationary, independent, and positive, we arrive at Equation 1:

$$\begin{aligned} \text{Outage Probability} = \Pr(W \leq L - M) &= \int_{-\infty}^{\infty} \Pr(L \rightarrow x) \Pr((W \leq \ell - M)|_{\ell=x}) dx \\ &= \int_{-\infty}^{\infty} f_L(x) F_W(x - M) dx \\ &= \int_M^{MaxWind} f_L(x) F_W(x - M) dx + \int_{MaxWind}^{\infty} f_L(x) dx \end{aligned}$$

Equation 1.

Figure 5 illustrates how Equation 1 captures the intuitive notion that increasing reserve margin will reduce outage probability. An increase in reserve margin causes $F_W(x - M)$ to shift to the right, which reduces the “overlap” between $F_W(x - M)$ and $f_L(x)$. Note that as it is drawn, Figure 5 represents a scenario with relatively high wind

penetration. At lower penetrations of wind, $MaxWind$ will decrease and the $F_W(x - M)$ curve will become “steeper.”

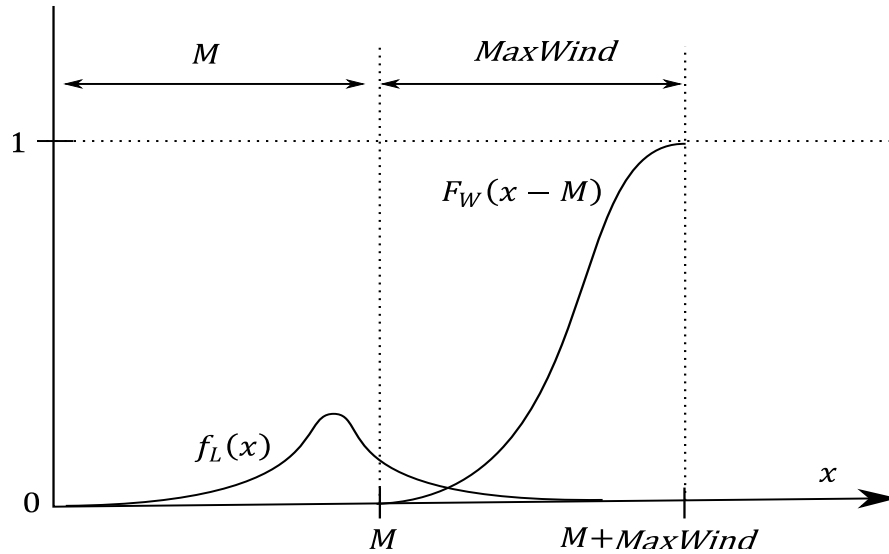


Figure 5. Relating reserve margin to wind and load statistics

Now, consider the effects of increasing the penetration of wind, by defining a new random process $W' = W + W_{new}$, where W_{new} is a stationary, independent and positive random process representing the additional wind power added to the grid. Employing a derivation similar to that used to obtain Equation 1, we arrive at Equation 2:

$$F_{W'}(x) \equiv \Pr(W' \leq x) = \int_0^{MaxNewWind} f_{W_{new}}(y) F_W(x - y) dy$$

Equation 2.

In this case, $F_{W'}(x)$ is the cumulative probability distribution function of W' , $f_{W_{new}}(y)$ is the probability density function of W_{new} , and $MaxNewWind$ is the additional installed wind generation capacity, beyond the existing wind generation

capacity. To simplify calculations, let us consider the first-order Taylor-series approximation of $F_W(x - y)$ in the neighborhood of x .

$$F_W(x - y) \approx F_W(x) - yF_W'(x) = F_W(x) - yf_W(x)$$

Equation 3.

Let $D(y) = \int_{-\infty}^{\infty} |F_W(x - y) - (F_W(x) - yf_W(x))| dx$ be a measure of the total distortion introduced by the approximation of Equation 3. Figure 6 shows that if we consider $F_W(x)$ to be a piecewise linear curve, then

$$D(y) = \frac{y^2}{MaxWind}$$

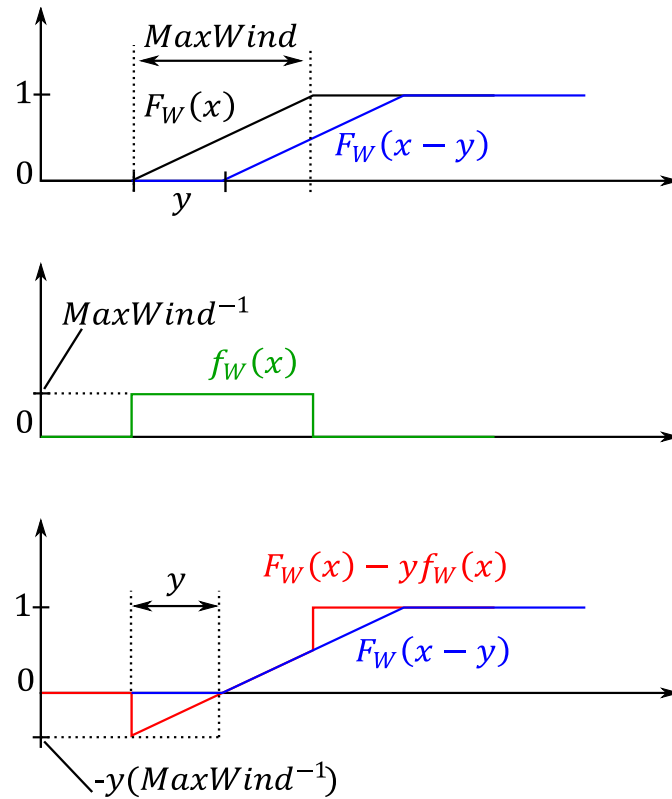


Figure 6. Taylor series approximation of cumulative distribution function

The approximation of $F_W(x)$ as a piecewise linear curve is valid if $F_W(x)$ is sufficiently “steep,” which translates to a low penetration of wind (see Figure 5). For the distortion $D(y)$ to remain small, y must be small in relation to $MaxWind$. This will remain true if the additional increment of wind is smaller than the total installed wind capacity ($MaxNewWind \ll MaxWind$). Now, plugging in the approximation of Equation 3 into Equation 2, we arrive at Equation 4:

$$\begin{aligned}
 F_{W'}(x) &\approx \int_0^{MaxNewWind} f_{W_{new}}(y)(F_W(x) - yf_W(x))dy \\
 &= \int_0^{MaxNewWind} f_{W_{new}}(y)(F_W(x) - yf_W(x))dy \\
 &= F_W(x) \int_0^{MaxNewWind} f_{W_{new}}(y)dy - f_W(x) \int_0^{MaxNewWind} y f_{W_{new}}(y)dy \\
 &= F_W(x) \times 1 - f_W(x)E[W_{new}]
 \end{aligned}$$

Equation 4.

In this case, $E[W_{new}]$ represents the expected value (mean) of the additional installed wind power. Applying the Taylor-series approximation again in reverse to Equation 4, we see that

$$F_{W'}(x) \approx F_W(x) - f_W(x)E[W_{new}] \approx F_W(x - E[W_{new}])$$

This analysis suggests that the decrease in reserve margin under small wind penetrations will be approximately equal to the mean of the added wind power. However, because we have assumed that the additional wind generation is “small” in comparison to the existing wind generation, we expect that this relationship will break down for large penetrations of wind. Finally, we also expect a further increase in reserve margin in real-life scenarios where the stationarity and independence assumptions of the wind and load do not hold.

Relationship between storage, demand response, and reserve margin.

To investigate the reserve margin effects of adding demand response and energy storage to the grid, we now consider the wind and load to be independent cyclostationary random processes $W(t)$ and $L(t)$ respectively. The effect of a dispatchable-load type demand response implementation with maximum time delay T will be to effectively low pass filter $W(t)$ – smoothing out power fluctuations of duration $\leq T$. Similarly, the effect of a storage implementation with capacity $E[W(t)]T$ will be to smooth the wind power fluctuations of duration $\leq T$. Figure 7 illustrates the process of demand response and energy storage, where the wind is given by a square wave with period $2T$.

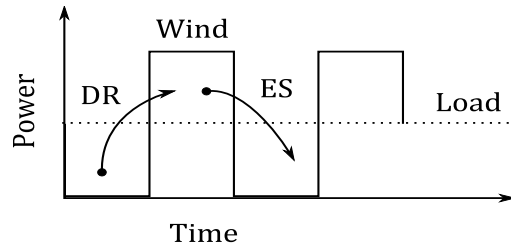


Figure 7. Illustration of demand response and energy storage

Now, let us define the “mixing time” of the wind power process as $T_{mix} = 1/q$ where q is the frequency below which lies most of the power of $W(t)$ ’s frequency spectrum. At $T < T_{mix}$, energy storage and demand response are not likely to have a measureable effect on reserve margin reduction. Furthermore, because the spectral power of $W(t)$ decreases rapidly with increasing frequency¹, T_{mix} is expected to be quite large on the time scale of interest. In particular, if we assume a $W(t)$ follows a Kolmogorov

¹ Meteorologically, the wind speed profile is made up of vortices of different energy and size. Larger vortices correspond to longer periods of fluctuation. Kolmogorov’s classic 1941 paper showed that the energy contained in turbulent vortices of non-viscous fluids (such as wind) decreases by an exponent of 5/3 as the period of fluctuation decreases [20]. Moreover, studies such as [21] demonstrate empirically that the Kolmogorov energy spectrum for wind speed can also be applied to extracted wind power.

spectrum and that the τ_{max} is longest-duration wind power fluctuation, then the power contained in fluctuations of duration greater than τ is given by

$$Q(\tau) = C \int_{1/\tau_{max}}^{1/\tau} f^{-5/3} df = \frac{3}{2} C (\tau_{max}^{2/3} - \tau^{2/3})$$

where C is a proportionality constant. The ratio $Q(\tau)/Q(0)$ represents the percentage of total power contained in fluctuations of duration greater than τ , and is given by

$$\frac{Q(\tau)}{Q(0)} = 1 - \left(\frac{\tau}{\tau_{max}} \right)^{2/3}$$

Assuming that $\tau_{max} \approx 1$ year, then 90% of the power is contained in fluctuations of duration greater than about 300 hours. On this time scale, we do not expect demand response to have a significant impact at delay limits of less than around 300 hours. Similarly, we expect energy storage to play a minor role until the capacity reaches almost two weeks of mean wind.

Hypotheses

In light of this cursory analysis, we present six hypotheses for investigation. These hypotheses are listed in Table 2.

Initial Hypothesis	Result
1. Reserve margin reductions are close to the mean wind at low wind penetrations	True
2. Degree of reserve margin reductions will decrease with increasing wind penetration	True
3. High correlation of wind power with itself and with load both have a negative impact on reserve margin reduction	True
4. Geographic distribution of wind turbines result in a reduction of correlation and therefore increased suitability for reserve margin reduction	True
5. Benefits of demand response and energy storage are minimal at low deployment	True
6. Energy storage capacity of T hours of mean wind power is roughly equivalent to demand response delay limit of T hours.	False

Table 2. List of hypotheses

Source Name	Credit/URL	Wind Speed	Wind Power Output	Load
NREL Eastern Wind Dataset	http://www.nrel.gov/wind/integration/datasets/eastern/data.html	1518 Sites 157968 samples each 2004-2006, Sited, Interpolated from measured data, 10min	1518 Sites 157968 samples each 2004-2006, Sited, Simulated IEC Class I, II, and III turbines, 10min	
Haina wind farm Dataset	Haina wind farm, Dominican Republic	1 Site 38775 samples 2010-2011, 80m wind speed, 10min	Simulated (piecewise linear power curve, class III turbine)	
MISO Historical Market Reports	https://www.midwestiso.org/Library/MarketReports/Pages/MarketReports.aspx		~300 Sites 38640 samples 2009-2012, Aggregate, Measured, Hourly	21120 samples 2009-2012, Measured, Hourly
AESO Public Data	http://www.aeso.ca/gridoperations/20544.html		~50 Sites 420768 samples 2011, Aggregate, Measured, 10min	420768 samples 2011, Measured, 10min
National Grid UK	http://www.nationalgrid.com/uk/Electricity/Data/Demand+Data/			194304 samples April 2001-April 2012, Measured, Half-hour

Table 3. Table of real-world information sources

Source Name	Credit	Wind Speed	Wind Power Output
Synthetic Random Field Model	Qiang Guo, Iowa State University for design and Matlab implementation	16761600 samples, Arbitrary time period, 1 second data, interpolated from actual 10m wind data and surface roughness parameters using Markov chain approach	Simulated (piecewise linear power curve, class II)
Sandia 3D Turbulence Model	P.S. Veers, for design and Francesco Perrone, for Matlab implementation.	12000 samples, Turbulence model based on PSD of measured data. 1 second data. Uses Von Karmen power spectrum method.	Simulated (piecewise linear power curve, class II)
Stationary Wind Model	self	38775 samples, Stationary random variable chosen from Weibull distribution with same mean and standard deviation as observed in Haina wind farm Dataset	Simulated (piecewise linear power curve, class II)
Filtered Gaussian Model	self		185684 samples, simple truncated Gaussian random variable (mean, standard deviation = 10), applied to a linear filter obtained from power spectrum of aggregate NREL dataset. (similar in idea to the Van Der Hoven Model)

Table 4. Table of simulated wind power sources

The remainder of this section details the methods which were used to test these hypotheses. These methods include the design of a first-principles simulation framework for reserve margin calculations, along with the development of software tools for validation, preprocessing, statistical comparison, and spectral analysis of real-world and simulated wind and load profiles. In the process, we discovered a number of results which were not directly related to our initial hypotheses. These results, including the

design of a new wind power simulation model, are presented alongside the descriptions of the research methods of this thesis.

Data Collection and Preprocessing

The first step in the testing of our hypotheses was to locate, validate, collate, and preprocess real-world load data, along with real-world and simulated wind data. Significant efforts were made to ensure a consistent and error-free comparison between the datasets. As a part of the data validation, we analyzed the effects of detrending, verified the spectral and long-term statistical characteristics of the NREL wind datasets, and discussed the decorrelation effects of linear filtering of wind power and load time series.

Data Sources

Table 3 and Table 4 provide the details of the real-world and simulated datasets which were obtained for this study. The following discussion outlines the key characteristics that were discovered by initial analysis of the data.

Preprocessing Flow

Before each power dataset could be input into the model, it was necessary to perform the preprocessing flow shown in Figure 8 in order to obtain consistent data. A two-step detrending procedure was performed on the grid-obtained data, to remove the effects of demand growth rate and rate of wind energy integration. Figure 9 illustrates the detrending procedure, which removes linear growth in mean load and the linear growth in peak wind generation, while maintaining the initial ratio of mean to peak variation. As would be expected, the effect of the detrending was a uniform reduction in the magnitudes of the frequency response.

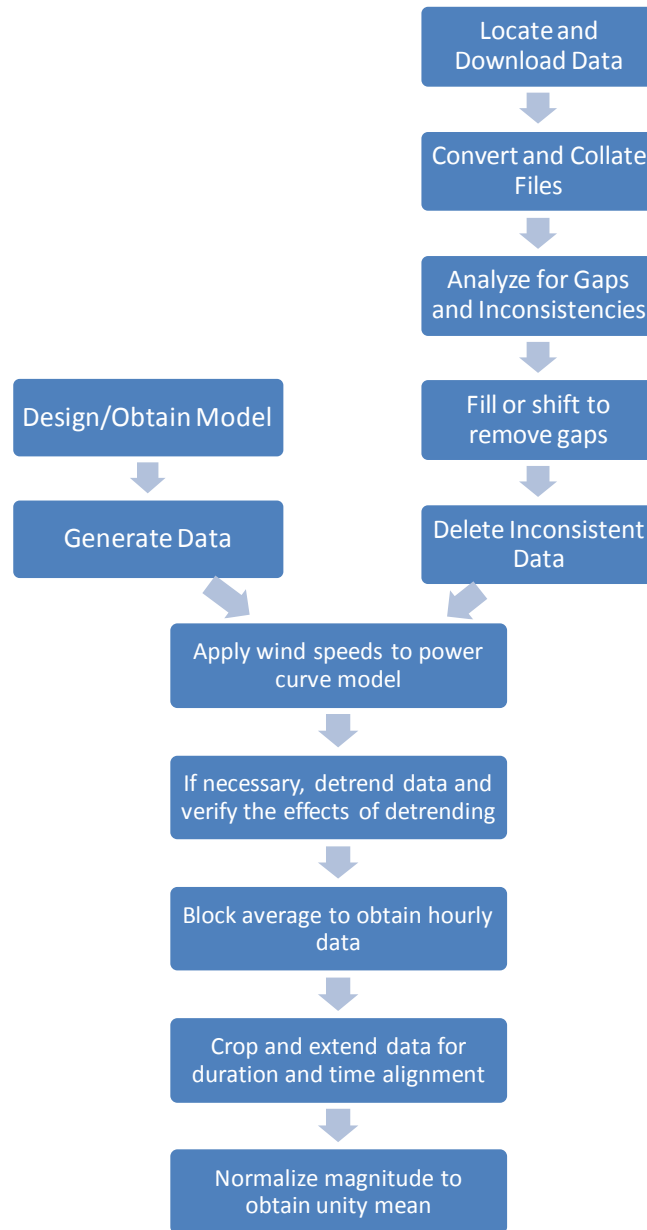


Figure 8. Preprocessing flow for real-world and simulated datasets

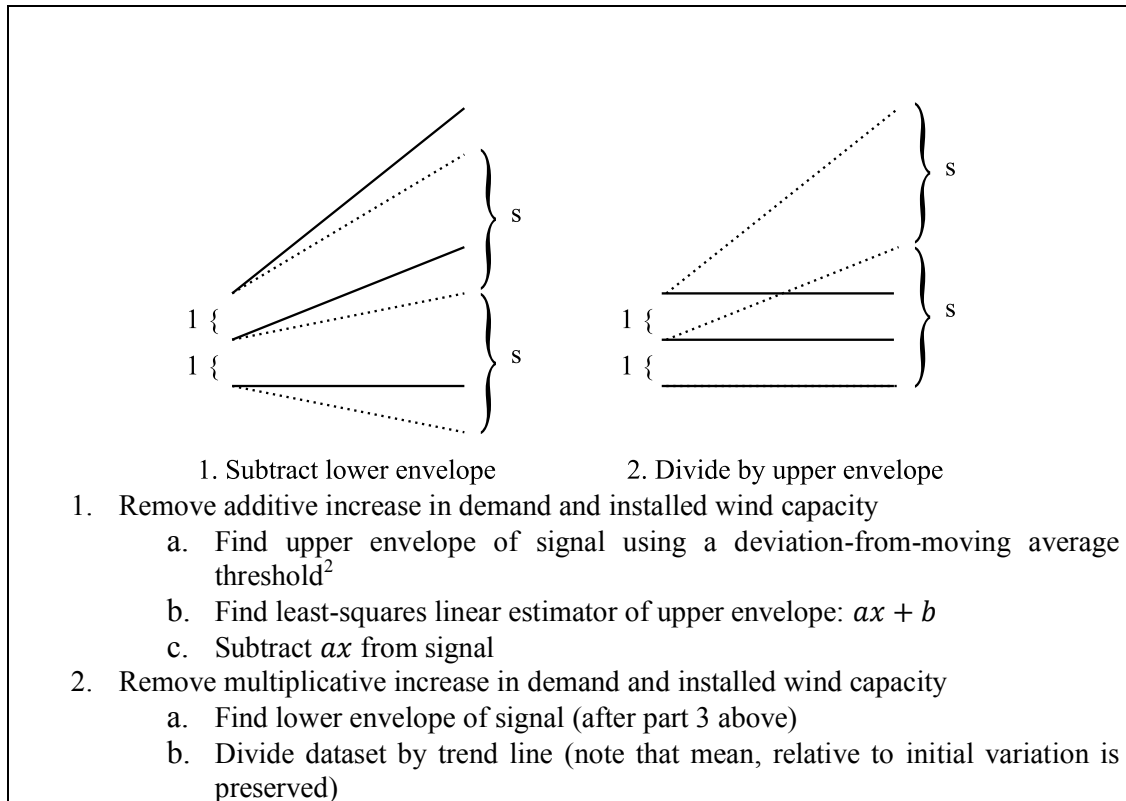


Figure 9. Detrending procedure

While higher-frequency data was available for some of the datasets, consistent comparison required that each dataset be normalized to the “lowest common denominator” sample time. In this particular case, each dataset was block-averaged to form hourly samples. Because the spectral power decreases with increasing frequency, it is likely that the effects of block averaging on reserve margin calculations will be minimal. However, it should be noted that, due to the limitations of the real-world datasets, this thesis only considers time scales greater than one hour.

After the data was averaged, the maximum-length segment representing a whole number of years was repeated a number of times and shifted such that the alignment difference (as measured by the absolute difference of the normalized and extended

² Detection of the lower and upper envelopes was accomplished by first computing the moving average of the sample using local regression (Lowess method). Peaks were then detected as locations which met particular level of deviation above and/or below the moving average.

datasets) between all datasets was minimal. This alignment procedure was necessary so that phase differences between the periodic cycles of the datasets did not skew our results. The number of repetitions required was determined by the length of the longest hourly dataset. Finally, each dataset was scaled to have unity mean, in order to aid calculations.

A summary of the important dataset parameters (before preprocessing) is given in Table 5. This table shows the observed increase in installed wind capacity for MISO and AESO and the observed change in total demand for MISO, AESO, and NG. Interestingly, the MISO load tended to decrease at a rate of 4.5 GWh/year, rather than increasing.

Dataset	Mean (MW)	Min (% of mean)	Max (% of mean)	Growth Rate of Weekly Minimum (MWh/year)	Growth Rate of Maximum Weekly Variation (MWh/year)	Sample Size	Sample Time (seconds)
NREL Wind Power	261387.9	6.97	211.98	0	0	157968	600
MISO Wind Power	2183.3	-4.13	279	98.97	1201.56	38664	3600
AESO Wind Power	148.88	-22.27	341.39	0.76	59.34	420768	600
Haina Wind Power	0.73	0	246.81	0	0	38775	600
MISO Load Power	63722.15	58.97	166.95	-4523.74	-2740.53	21120	3600
NG Load Power	37536.94	53.08	161.62	227.71	184.88	194304	1800
AESO Load Power	7925	75.65	126.29	106.79	25.21	420768	600

Table 5. Summary of raw dataset parameters

Descriptions and Discussion of Individual Datasets

NREL Eastern Wind Dataset

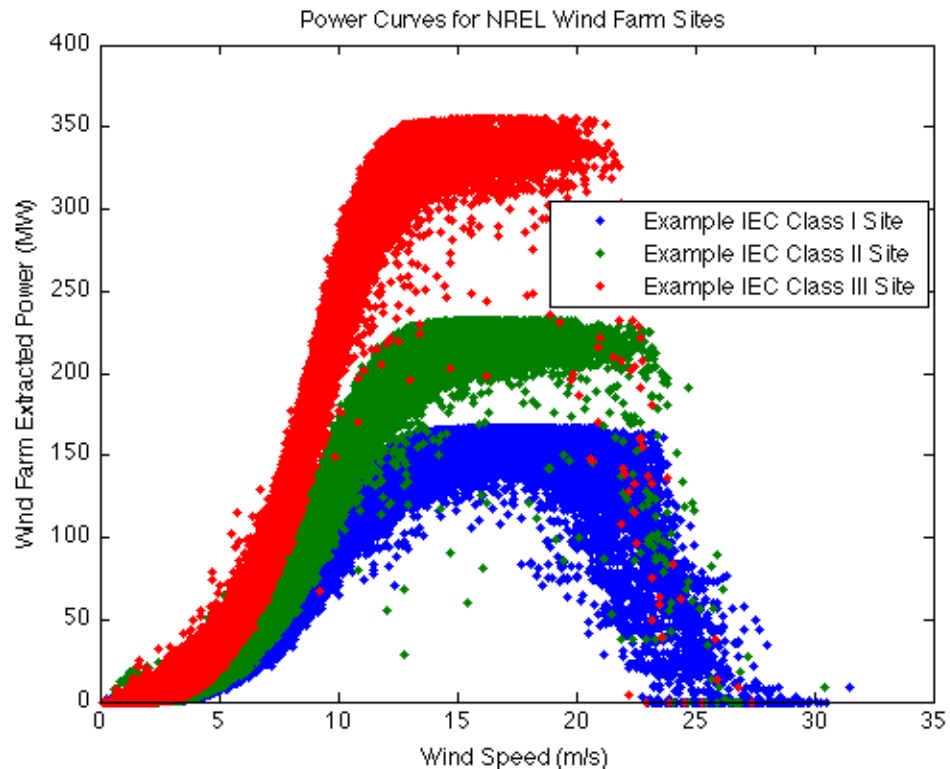


Figure 10. Wind farm power extraction curves for three example sites corresponding to high (Class I), medium (Class II) and low (Class III) wind speeds.

The NREL Eastern Wind Dataset is a collection of 3 years worth (2004-2006) of 10-minute simulated wind conditions at 80 and 100 meters, for 1518 potential wind farm sites across the Midwestern and Eastern United States. AWS TrueWind produced the wind speed data by inputting measured met-tower data into a meteorological model, and geographically interpolating to desired wind turbine locations. The wind speed listed represents an average of the wind speeds at several individual turbine locations. The NREL study input the wind speed data into models for three different class turbines (designed for IEC class I, II, and II, corresponding to high, medium, and low wind speed

conditions), and selected the optimal turbine for maximum power extraction during the period of study. The IEC class I and II turbines were placed at 80 meters, and the IEC class III turbines were placed at 100 meters. The dataset does not include individual turbine power extractions, but rather wind farm power outputs. An example power curve of the IEC class III turbine is in Figure 10. Notice that the dataset includes wind farms of different installed capacity.

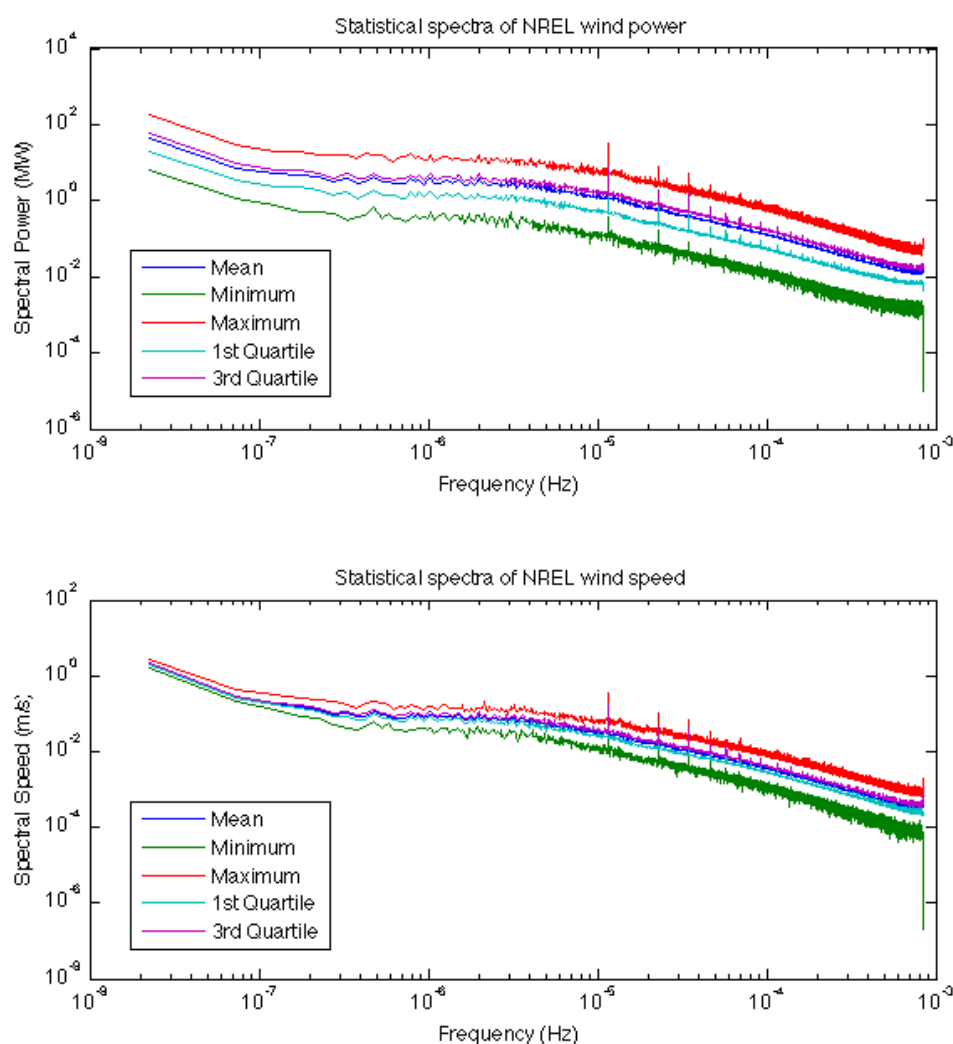


Figure 11. “Box plot” of power and speed in the frequency domain, showing the minimum and maximum spectral components, along with the mean, 1st and 3rd quartiles.

The dataset used in this thesis represents an aggregate of all 1518 wind power time series, and contained no gaps or invalid timestamps. Figure 11 shows that the spectral characteristics remained consistent throughout the datasets, agreeing with the results of [21]. This figure was obtained by generating the frequency spectrum of each wind power time. The frequency spectrum was block-averaged by 8 frequency samples in order to reduce memory requirements.

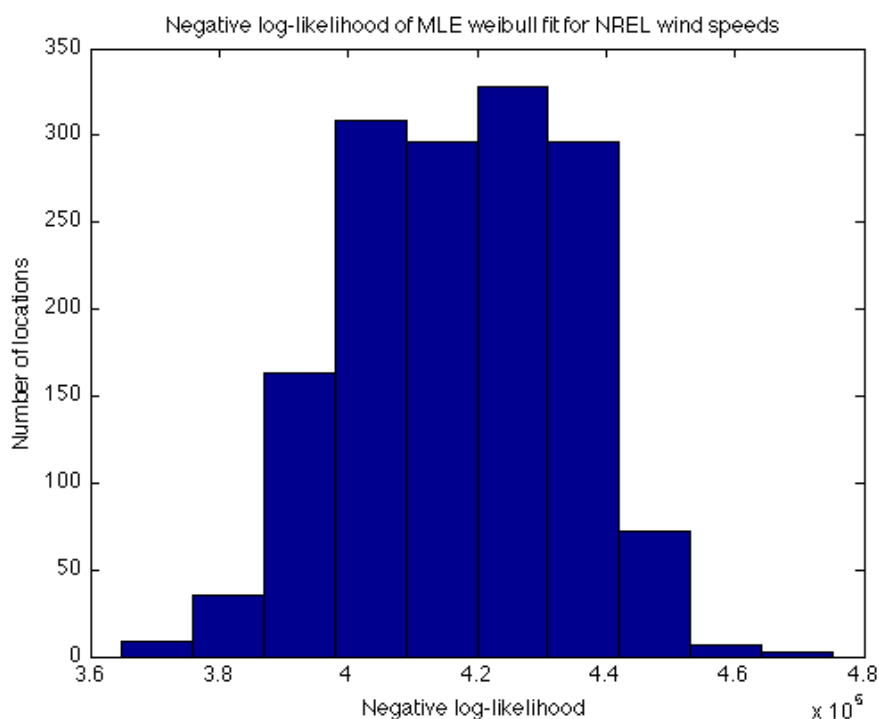


Figure 12. “Goodness of fit” analysis, demonstrating that the datasets followed a Weibull distribution in their long-term characteristics.

To better understand the variations involved, the long-term probability characteristics (100-bin histograms) were obtained for each dataset. Figure 12 is a “goodness of fit” analysis of the NREL wind speed dataset, as compared to the Weibull distribution, which is the well-accepted standard [17] distribution for long-term wind speeds. For comparison, it should be noted that the negative log likelihood of the MLE

Weibull fit for a the positive values of a truncated Gaussian dataset with mean 10 and standard deviation 10 is approximately 3×10^4 , an order of magnitude smaller than the minimum negative log likelihood calculated for this dataset.

Figure 13 is a probability map of the wind power and wind speed. This plot accurately reflects the fact that areas of high average wind speed are prone to large variability in wind speed, and thus highly-variable power output. Color represents the probability of observing a particular wind speed. The colors in the power plot have been scaled logarithmically to highlight the variations at small probability.

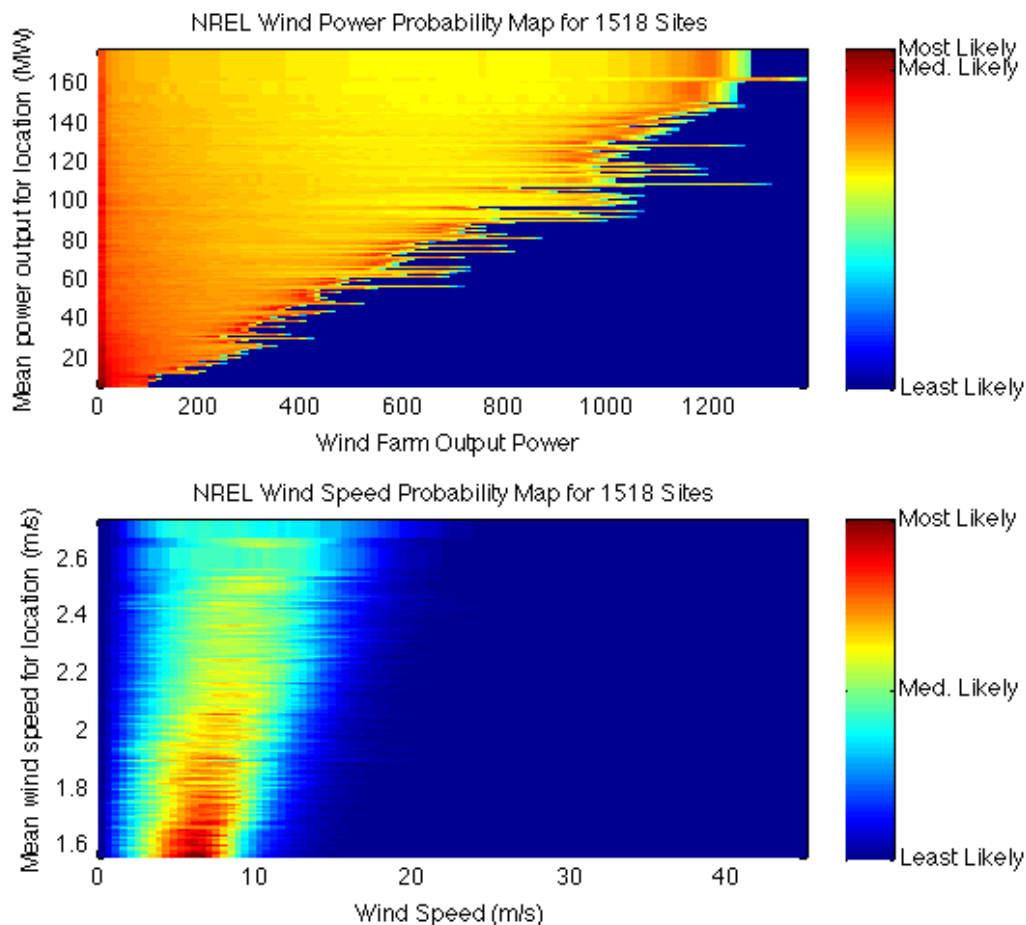


Figure 13. Long term probability map of site data. The y axis represents the site characteristic (mean wind speed or power), the x axis represents observed wind speed or power.

Haina wind farm Dataset

The Haina dataset was generously provided by the EGE Haina wind farm in the Dominican Republic. There were nine gaps in the data, shown in Table 6. These gaps were expanded to coincide with an exact number of days, for more accurate spectral variation. In each gap-adjustment instance, 72 samples removed from the beginning of each gap so that there is a transition from 23:50:00 to 00:00:00, instead of a transition from 01:50:00 to 00:00:00.

Number of gaps	Gap duration	Corrected gap duration
1	27 days, 23 hours, 10 min	28 days
7	23 hours, 10 min	1 day
1	6 days, 23 hours, 10 min	7 days

Table 6. Haina wind gap information

Figure 14 and Figure 15 demonstrate the benefit of this procedure, by comparing the autocorrelations and frequency spectra of the original and gap-adjusted data with those of the largest section of 10minute wind data without gaps (corresponding to 24060 samples). In each case, the adjusted data was shown to be more similar to the no-gap data than the non-adjusted data was.

The Haina wind speed dataset was converted to a wind power dataset via a piecewise linear power curve corresponding to the Vestas V100-1.8 MW GridStreamer turbine. This turbine was selected among the eleven (2 MW or less) turbines available from Vestas because it produced the maximum capacity factor for the Haina wind speed dataset.

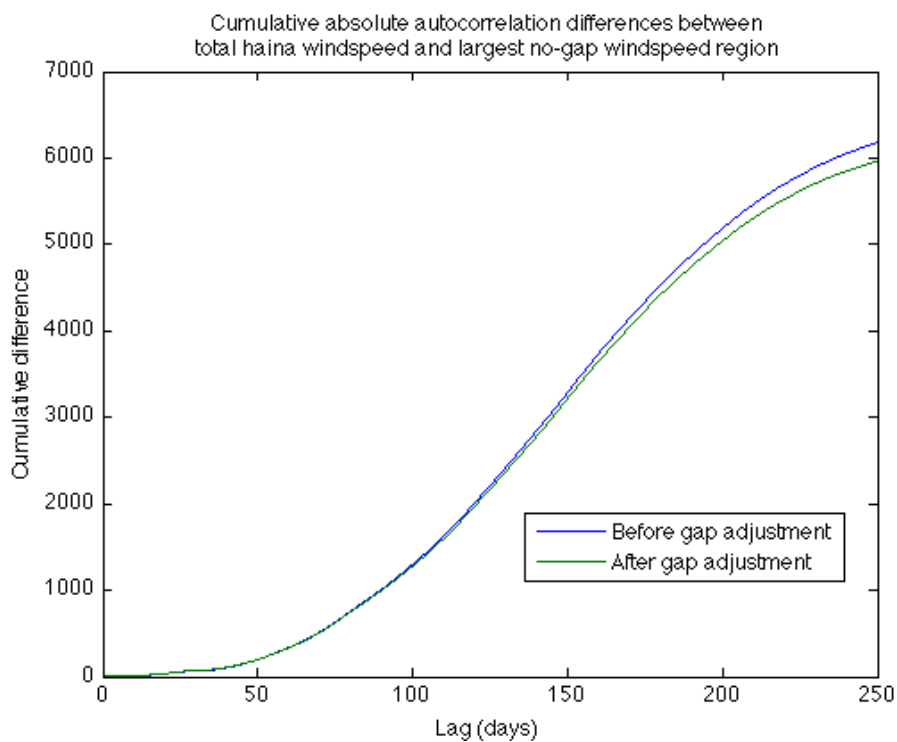


Figure 14. Differences between the autocorrelation functions of the no-gap data, with the gap-adjusted and non-adjusted data

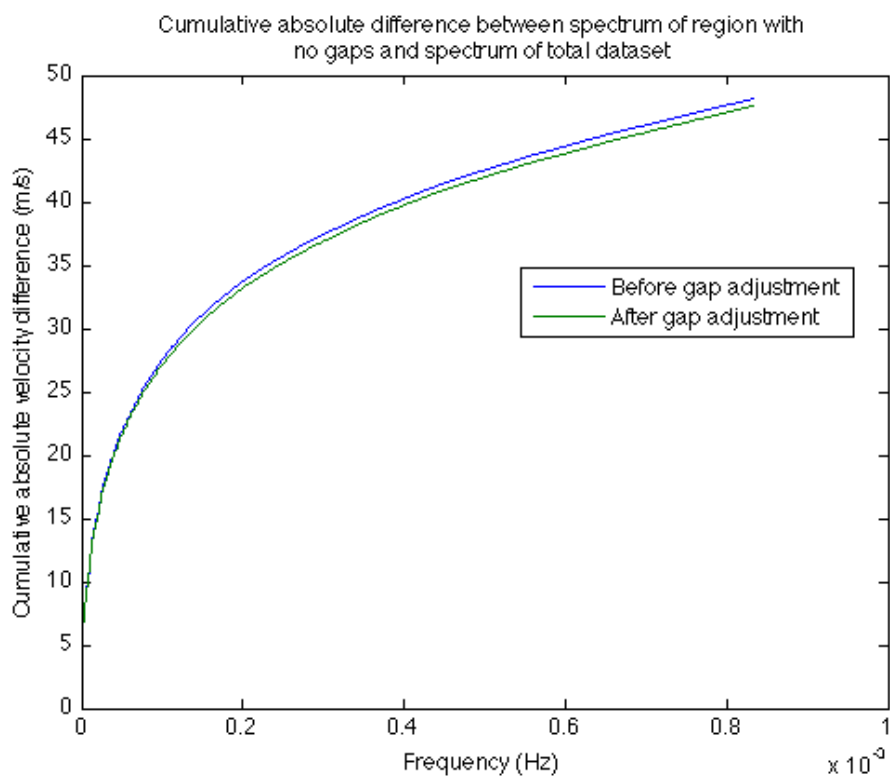


Figure 15. Differences between the spectral velocity of the no-gap data, with the gap-adjusted and non-adjusted data.

Turbine Height (m)	Rated Power (MW)	Cut-in speed (m/s)	Rated speed (m/s)	Cut-out speed (m/s)	Capacity Factor (% of Rated Power)
80	1.8	3	12	20	40.52

Table 7. Chosen turbine parameters for converting the Haina wind speed to power

Rated Power (MW)	Cut-in speed (m/s)	Rated speed (m/s)	Cut-out speed (m/s)	Wind-Class
850	4	16	25	IEC S
850	3.5	13	20	IEC IIB
2000	4	16	25	IEC IIA
2000	3.5	14.5	25	IEC IA
1800	4	12	25	IEC IIA
2000	4	12	25	IEC IIIA
1800	3.5	13	25	IEC IIA
2000	3.5	13.5	25	IEC IIIA
2000	4	13.5	25	IEC IA
1800	3	12	20	IEC S
2000	3	12.5	20	IEC IIA

Table 8. Turbine parameters for Vestas turbines, 2MW or less (obtained from [22])

MISO Historical Market Reports

The MISO Historical Market Reports dataset represents hourly aggregate wind and load information from the Midwest Independent System Operator. The most recent data represents an aggregate of approximately three hundred turbines, while the oldest data represents fewer aggregate turbines. There were no gaps in the hourly MISO data, however the dataset did require detrending. The results of this detrending process are detailed in Figure 16 and Figure 17. Table 5 on page 30 lists the detrending parameters for this and other datasets. Notice that the difference in spectra between the trended and

detrended data was not significant. The cumulative absolute spectral difference between original and detrended data was less than 3% of the total spectral energy for the load dataset and less than 20% of total spectral energy for the wind dataset.

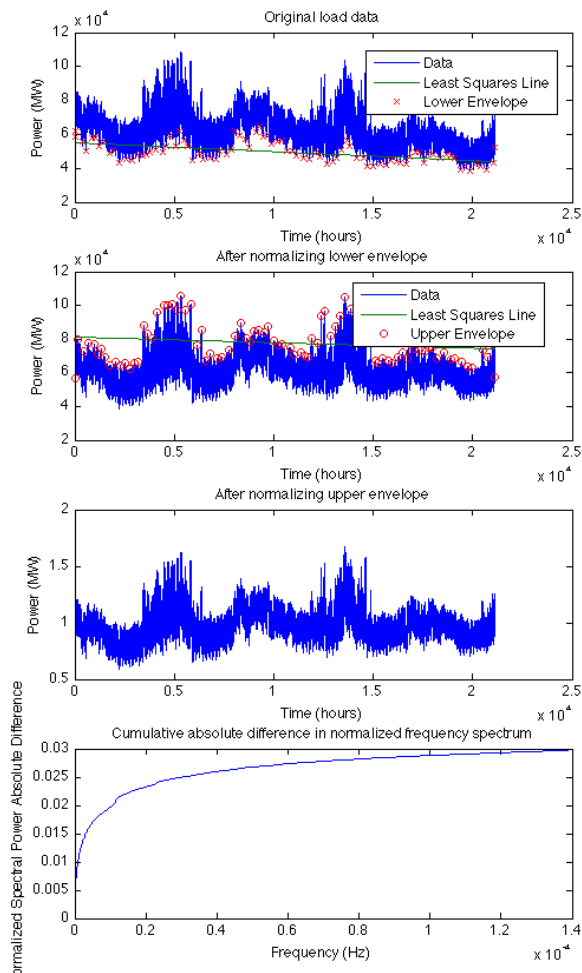


Figure 16. Detrending process for MISO load

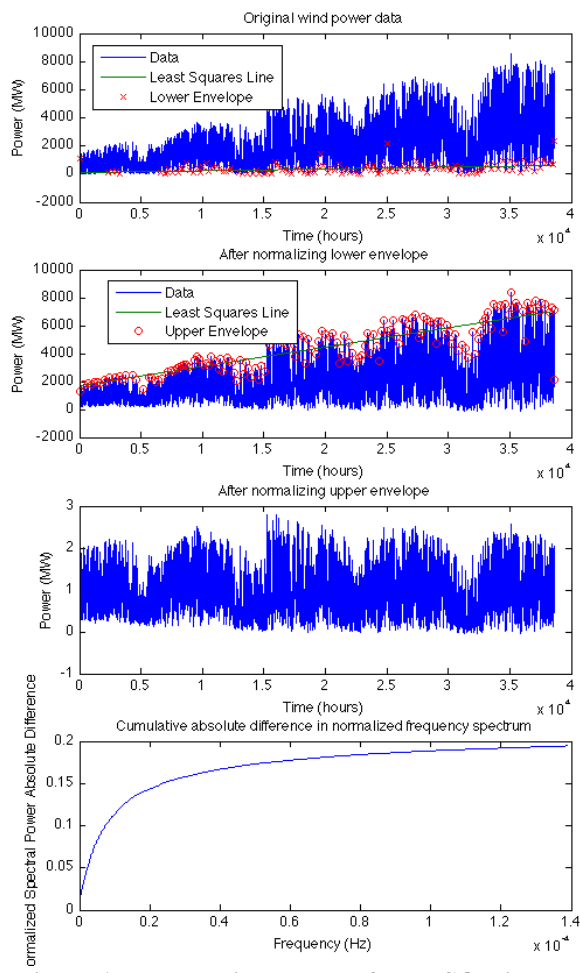


Figure 17. Detrending process for MISO wind

AESO Wind power / AIL Data

The most recent data in the AESO Wind power dataset represents cumulative wind power from around 50 wind farms, with the earlier data representing fewer farms. Similar to the MISO datasets, the AESO wind and load datasets required detrending. In

this dataset, there were eight 1-hour gaps in the 10 minute data. To avoid a half-day phase shift in the data across the course of the dataset, these gaps were filled by inserting a copy of the six samples prior to each gap. In addition to the eight data gaps, there were eight segments of data containing repeated timestamps. This extra data was discarded. The results of the gap-adjustment procedure and the detrending were similar to those observed in the Haina wind and the MISO datasets.

NationalGrid UK Demand Data

The NationalGrid UK demand dataset was the largest single dataset considered. This half-hourly dataset was similar to the AESO data, in that there were a number of gaps (10), and incorrect timestamps (22). The gaps were filled with previous samples, and the data points with incorrect timestamps were removed.

Synthetic Random Field Model

The synthetic random field model is a generated random field model developed by Quing Guo and Baskar Ganapathysubramanian at Iowa State University. The method extracts variation statistics from measured wind data and uses these to initialize a random walk, using a MCMC (Markov Chain Monte-Carlo) type approach. The model realization we were provided with generates wind speeds at 10 meters above ground, at one second intervals.

While an arbitrary number of samples could be generated, we generated only 194 days worth of data, due to time and memory constraints. This data was block-averaged to ten-minute data, which was then used to select a turbine from the same list as was used for the Haina dataset. The piecewise linear power curve of this turbine was used to generate power data.

Sandia 3D Turbulence Model

The Sandia 3D Turbulence Model was developed by P.S. Veers in 1988 for use in generating high frequency wind speeds [23]. The implementation we used was written by Francesco Perrone of AREVA Wind GmbH. The samples are generated at one second intervals, at a height of 80 meters. Due to time and memory constraints, only 50 days worth of data were generated. Conversion from wind speed to power was accomplished identically to the other simulated wind speed datasets.

Stationary Wind Model

The stationary wind model is nothing more than a stationary random variable (Weibull distribution) for wind speed, passed through a piecewise-linear power curve. The parameters for the Weibull distribution used were obtained by fitting the Haina wind speed data using maximum likelihood estimator. The number of data points generated was equal to the number of data points in the Haina wind dataset, and the turbine was chosen in the same manner as the other simulated wind speed datasets.

Filtered Gaussian Model

The filtered Gaussian model uses a method similar to [24] and others that compute random wind series from assumptions about the frequency domain characteristics (namely, that it follows a Kolmogorov power spectrum). However, this method does not attempt to reproduce turbulence characteristics or to reach any particular distribution in steady-state. The procedure is simply to filter Gaussian white noise (truncated to be strictly positive) with a comb-shaped filter defined by the spectral peaks of a training signal's spectrum and then to filter again with a low-pass filter defined by the moving average of the training signal's spectrum. Figure 18 illustrates the process.

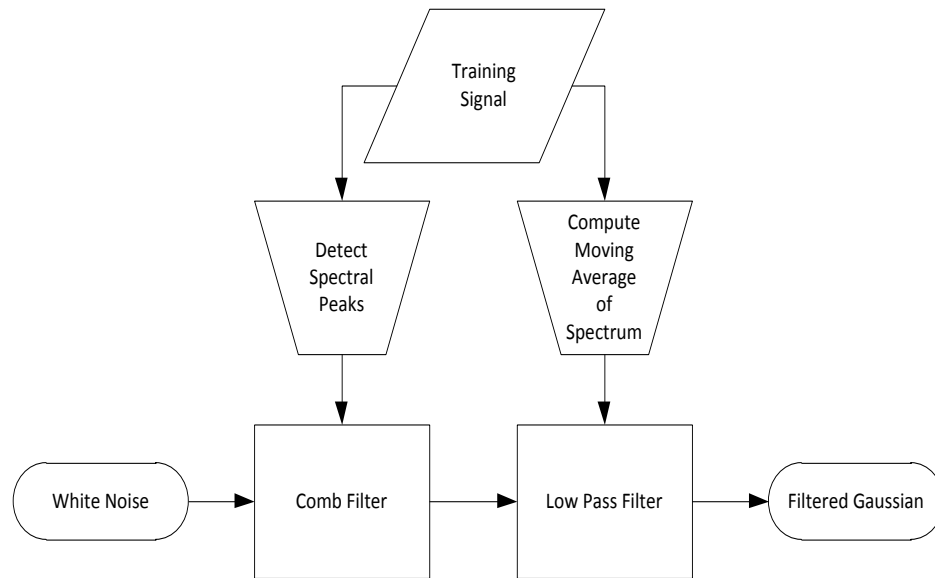


Figure 18. Process for Filtered Gaussian Model

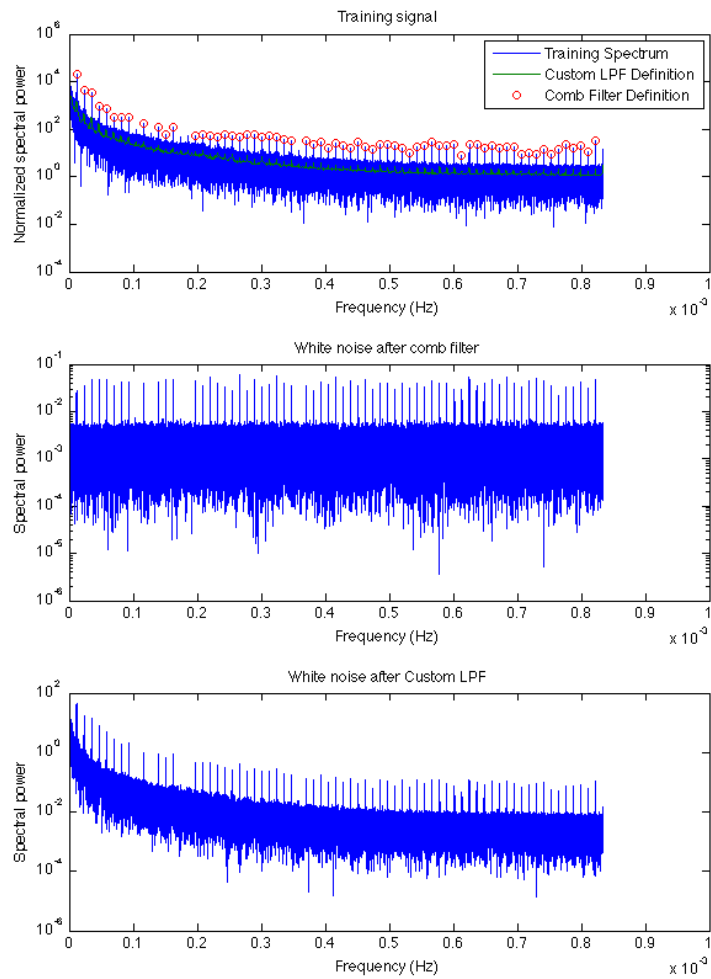


Figure 19. Illustration of filtering process

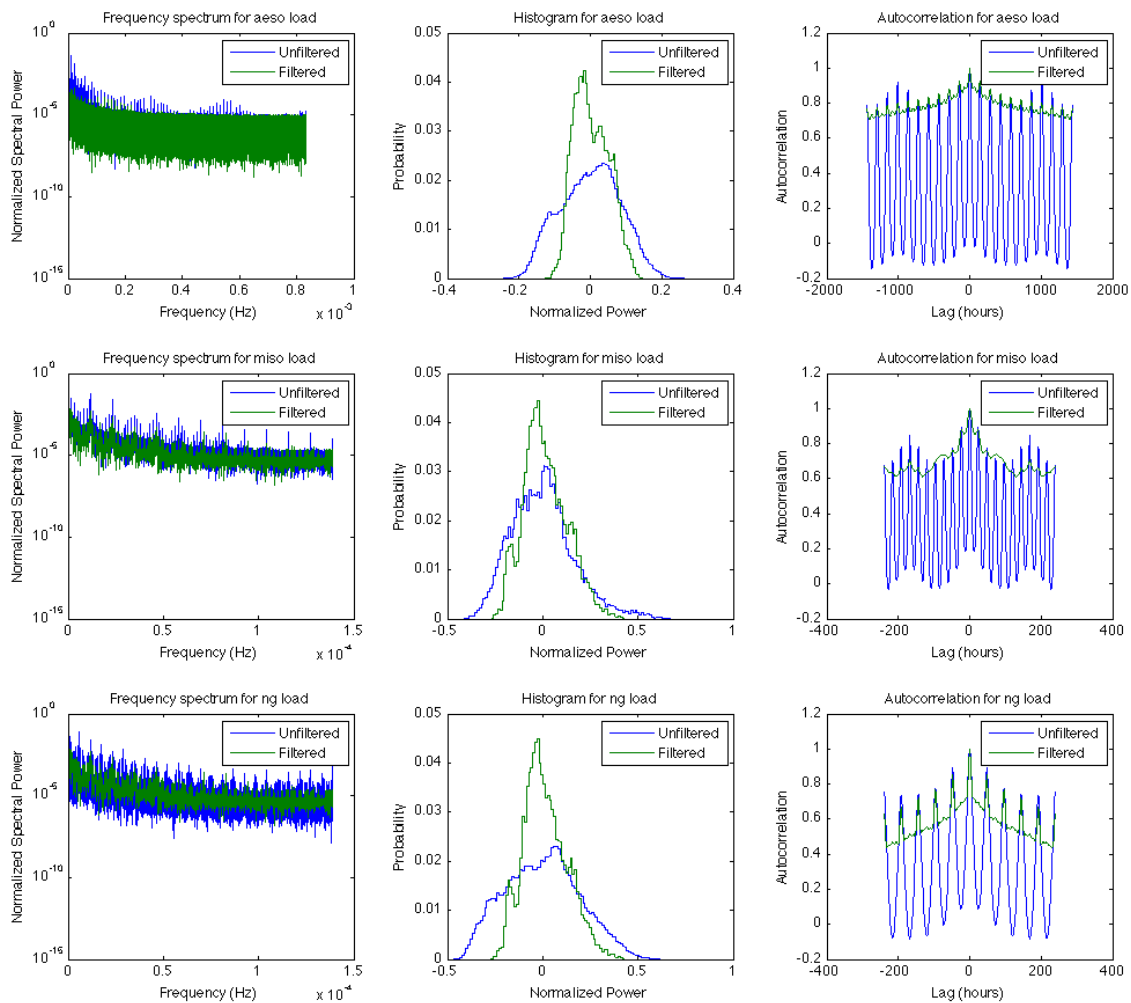


Figure 20. Load profile showing the effects of filtering spectral peaks.

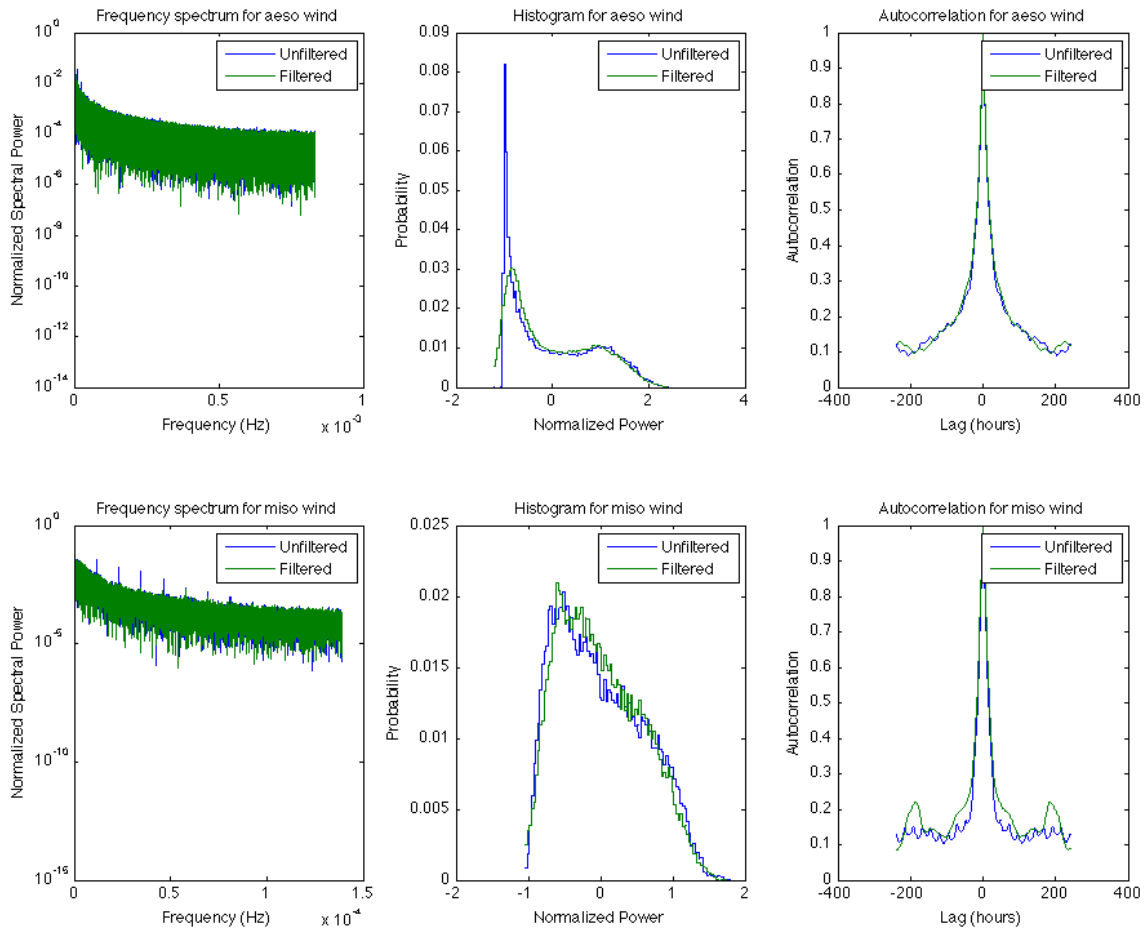


Figure 21. Wind profile showing effects of filtering spectral peaks.

The peak-finding algorithm was the same as was used to find the upper and lower envelopes for the detrending procedure. The training signal for our the filtered Gaussian time series was the NREL aggregate wind power dataset. Three years worth of data were generated in this manner.

Effects of predictable periodicity on autocorrelations

Motivation for this filtered stationary process wind power model came from our initial investigations into the cyclostationary nature of grid loads. As the Figure 20 illustrates, filtering out the obvious spectral peaks results in significant de-correlation of the grid load. Comparing the 10-day autocorrelation plots of the filtered and un-filtered loads, it is clear that the predictable behavior (i.e. that variation which results from the

spectral peaks) accounts for the majority of the non-stationarity of the load signal. The slope in autocorrelation is likely due to a low-frequency peak which was not detected. It was initially thought that wind power profile would respond in a similar fashion, given that the wind power spectrum also contains large peaks and that a filter which introduced these peaks into stationary data would accurately model the wind power variation.

However, Figure 21 illustrates that the power spectrum of wind does share this reduction in autocorrelation when the spectral peaks were filtered – most likely due to the fact that the spectral peaks of wind power are few and are not so pronounced as those in the load spectrum. This is what led us to also introduce a low-pass filter into the model in addition to the comb-type filter.

Simulation Architecture

The simulation architecture for model comparison is shown in Figure 22. Hourly wind generation data were scaled to achieve a desired penetration of wind energy. Penetration is defined as total energy generated from wind divided by the total load serviced by the grid. After reserve power requirements for 100% reliability were calculated individually at each time sample, the reserve power requirements were sorted into percentile bins, and the minimum reserve margin for 0.027% loss of load probability (LOLP) was calculated. Note that this model does not include generator ramp rates or other practical considerations, but instead was designed to study the fundamental reserve margin limits imposed by high wind penetrations.

In addition to calculating reserve power requirement, the following additional metric was calculated, which can be thought of as the “penetration benefit”:

$$\frac{\text{Decrease in Reserve Power}}{\text{Increase in Wind Penetration}}$$

The penetration benefit metric is comparable to the more commonly used intermittency-mitigation metrics of price elasticity and peak reduction [9]. However, in

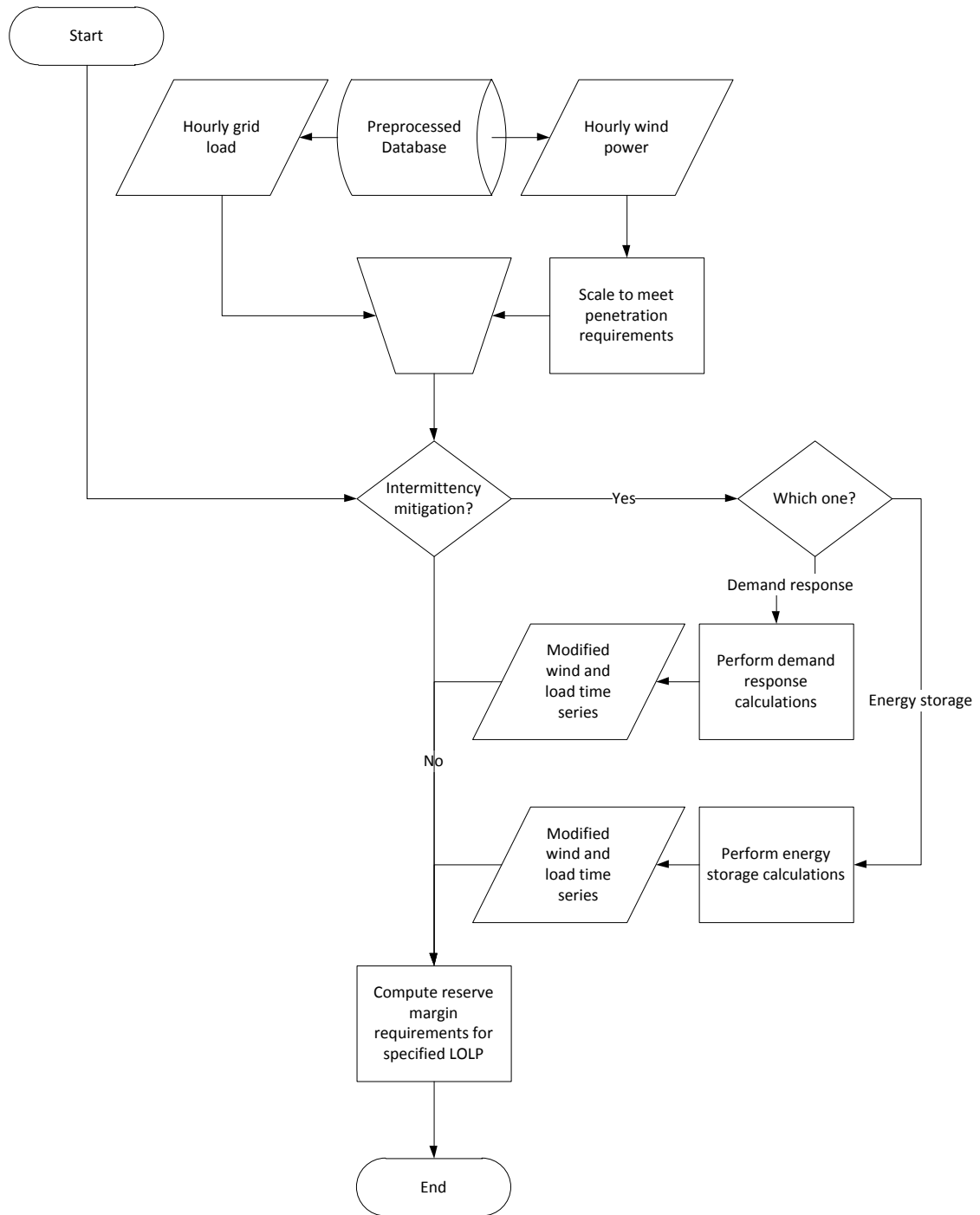


Figure 22. Simulation model overview

this particular study, a metric is desired for evaluating the relative benefit of “adding more wind turbines” in the presence or absence of grid reliability techniques like energy

storage and demand response. In particular, this metric is used to assess the first hypothesis of Table 2.

Idealized Energy Storage Device

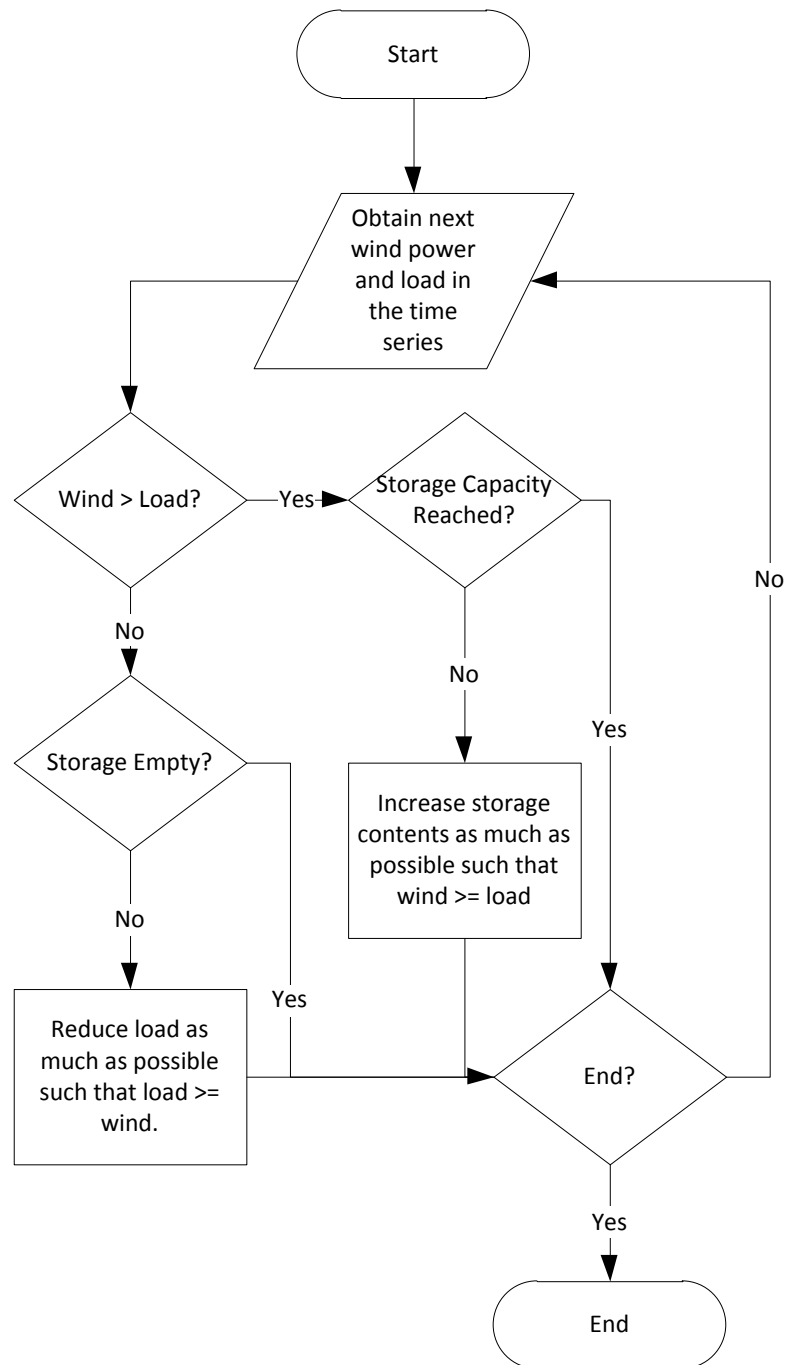


Figure 23. Algorithm for energy storage model

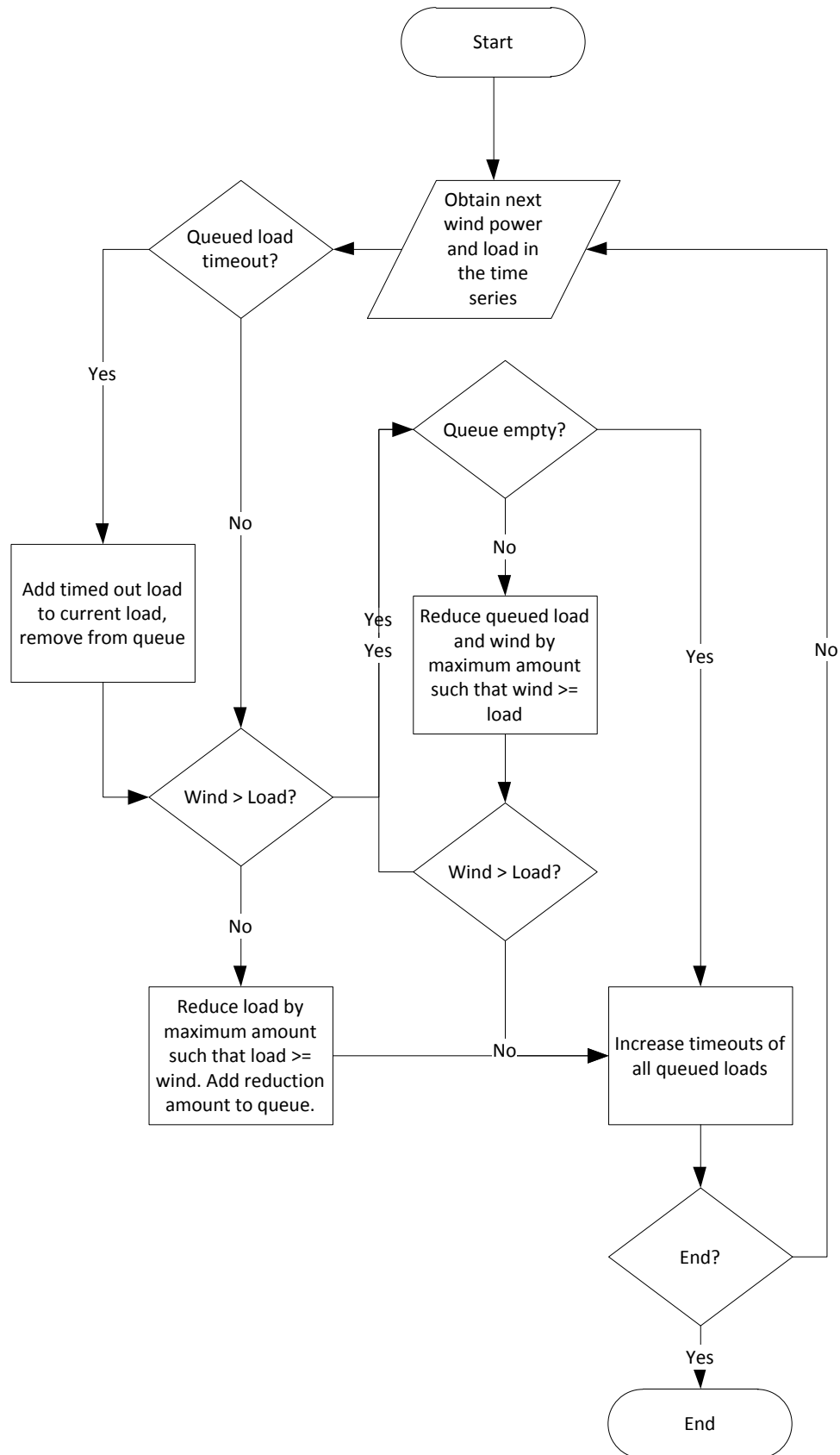


Figure 24. Algorithm for demand response model

Since the energy storage model is intended to simulate an ideal (fast ramp rate) technology, we ignore any hardware-imposed restrictions on rate of charge, discharge, or the duration that a charge may be held. However, because battery capacity is one of the aspects under investigation, we do place a limit on the capacity of charge that can be stored. The algorithm for the energy storage model shown in Figure 23 modifies the wind and load profile to reflect renewable-oriented dispatch priorities. If possible, the current demand is met via wind energy. If there is any extra wind power, it is used to charge the energy storage device. Energy storage is discharged to reduce reserve requirements when the wind is less than the load.

Idealized Demand Response

The queue-based demand response model is based on one of the less intrusive methods of demand shaping. It is assumed that no user will reduce his or her electricity consumption, but that he or she is willing to delay the electricity usage by a certain amount of time. The amount of delay time is limited to a maximum beyond which the grid must immediately service the delayed load. Finally, the queue is emptied in a first-come-first-serve (FIFO) manner in order to minimize the number of loads which “time out.” The algorithm for the demand shaping model is shown in Figure 24.

Results

Before presenting the results of our model analysis, we discuss how the the hypotheses made at the beginning of this chapter are to be tested and reiterate the primary assumptions associated with our simulation architecture.

The first and second hypotheses may be tested by simply computing the reserve margin reductions for a range of wind penetrations. The third proposition may be tested by comparing the auto- and cross-correlations of the load and wind power datasets with the results of the reserve margin reduction calculations. The fourth conjecture is

answered by computing the reserve margin reductions of wind power datasets across an increasingly large geographic area.

Initial Hypothesis	Result
1. Reserve margin reductions are close to the mean wind at low wind penetrations	True
2. Degree of reserve margin reductions will decrease with increasing wind penetration	True
3. High correlation of wind power with itself and with load both have a negative impact on reserve margin reduction	True
4. Geographic distribution of wind turbines result in a reduction of correlation and therefore increased suitability for reserve margin reduction	True
5. Benefits of demand response and energy storage are minimal at low deployment	True
6. Energy storage capacity of T hours of mean wind power is roughly equivalent to demand response delay limit of T hours.	False

Table 9. List of hypotheses

The fifth supposition may be verified by computing the reserve margin reductions of energy storage and demand response, compared to the reductions without intermittency mitigation. The sixth premise may be proven or disproven by a comparison of the reserve margin reductions produced by demand response with those generated from energy storage, under the same conditions.

As noted earlier in this chapter, the preprocessing steps and simulation architecture used in this thesis make a number of assumptions about the data and the grid under investigation:

1. The hourly reserve statistics are representative of the shorter time-period reserve margin calculations.
2. Detrending and repetition of load and wind power datasets does not distort reserve margin calculations.
3. There are no ramp rate restrictions on reserve or energy storage.

4. There is no maximum capacity for demand response – only a maximum time till service.
5. There is no maximum duration for energy storage – only a maximum storage capacity.

Effects of high wind penetrations on RMA

This section confirms hypotheses one through four with reserve margin simulations and a comparison of the auto- and cross-correlations of the various load and wind profiles.

Reserve Margin Calculations

As is shown in Figure 25 and Figure 26, the reserve margin reduction is shown to be close to 100% of the mean wind power at low wind penetrations – for each one of the real and simulated datasets. Thus, the first hypothesis is verified. Similarly, all but one simulation result in a substantial decrease in reserve margin reduction, with increasing wind penetration. The Sandia 3D model is the only case in which the reserve margin reduction remains close to 100% even at higher wind penetrations – indicating that this particular model adheres to the assumptions made in our analysis at the beginning of this chapter. It is also interesting to note that each dataset (with the exception of the Sandia model) reaches a relatively low potential for reserve margin decrease around 20% wind penetration, which corresponds to the 2030 wind penetration goal set by the U.S. Department of Energy.

The Synthetic Random Field simulation, which was intended to accurately model wind speed frequency characteristics up to one day, and the stationary wind speed model, which made no effort to reproduce frequency characteristics both performed similarly to the highly-aggregated NREL dataset. This result is consistent with [25], in that MCMC wind speed models tend to exhibit an inadequate level of correlation at longer time scales. However, this result also shows that high levels of aggregation tend to produce

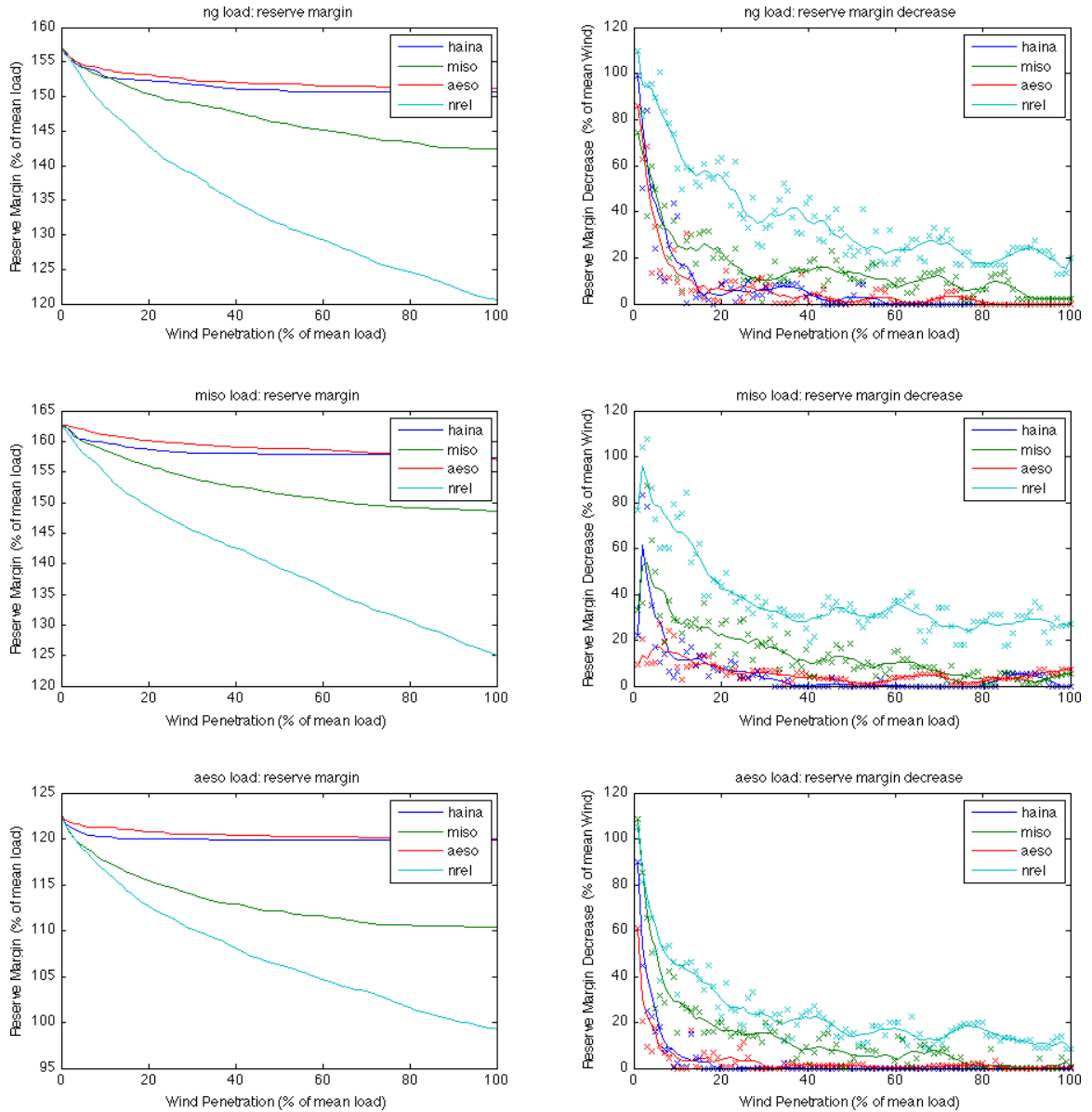


Figure 25. Reserve margin calculations for real-world wind generation data

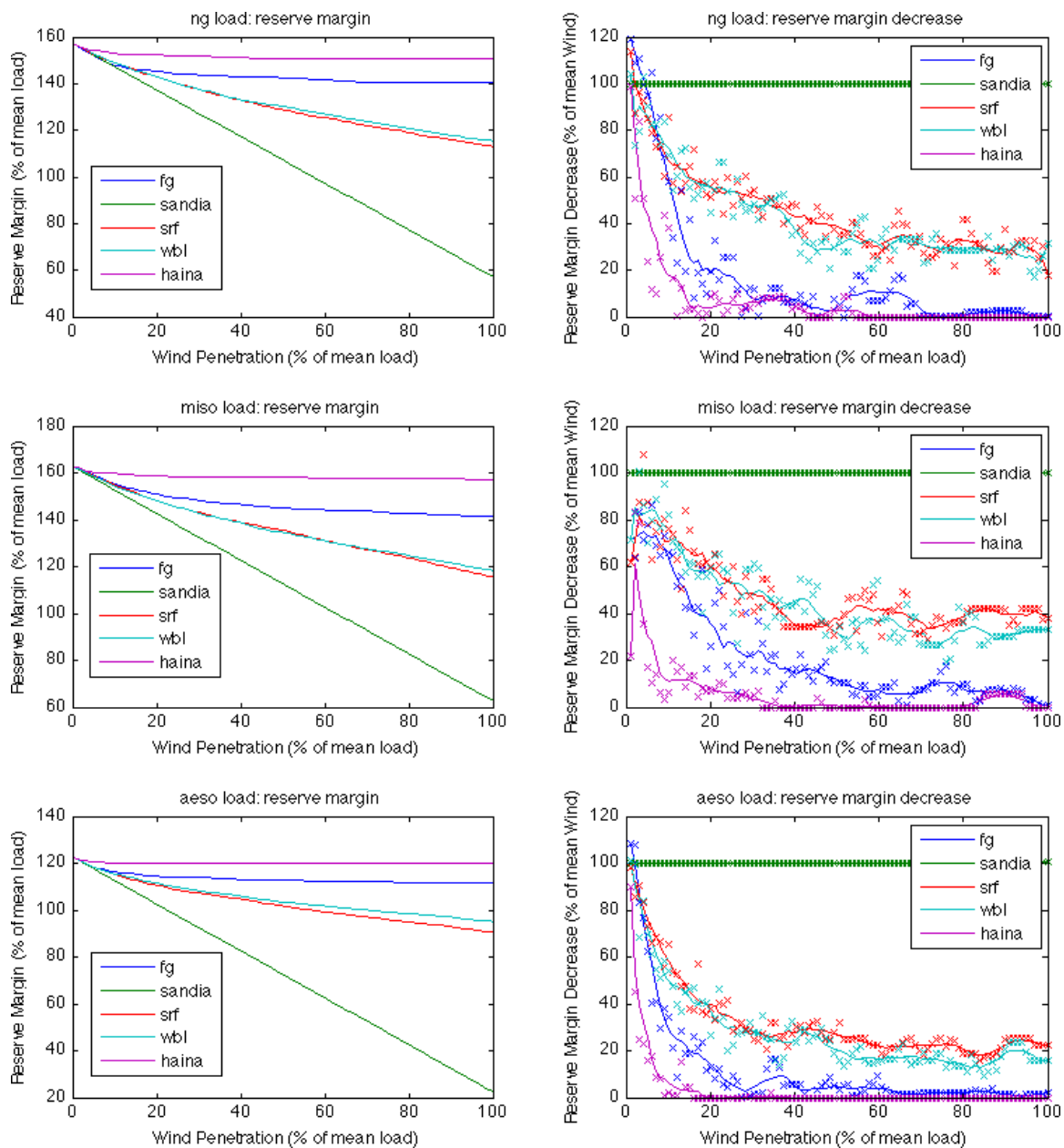


Figure 26. Reserve margin calculations for simulated wind data

power profiles which are statistically similar to a stationary random process. The filtered Gaussian wind power model produced a reserve margin reduction profile that more accurately reflected the sharp decrease in reserve margin reduction that is observed in the dataset produced from real-world wind (Haina).

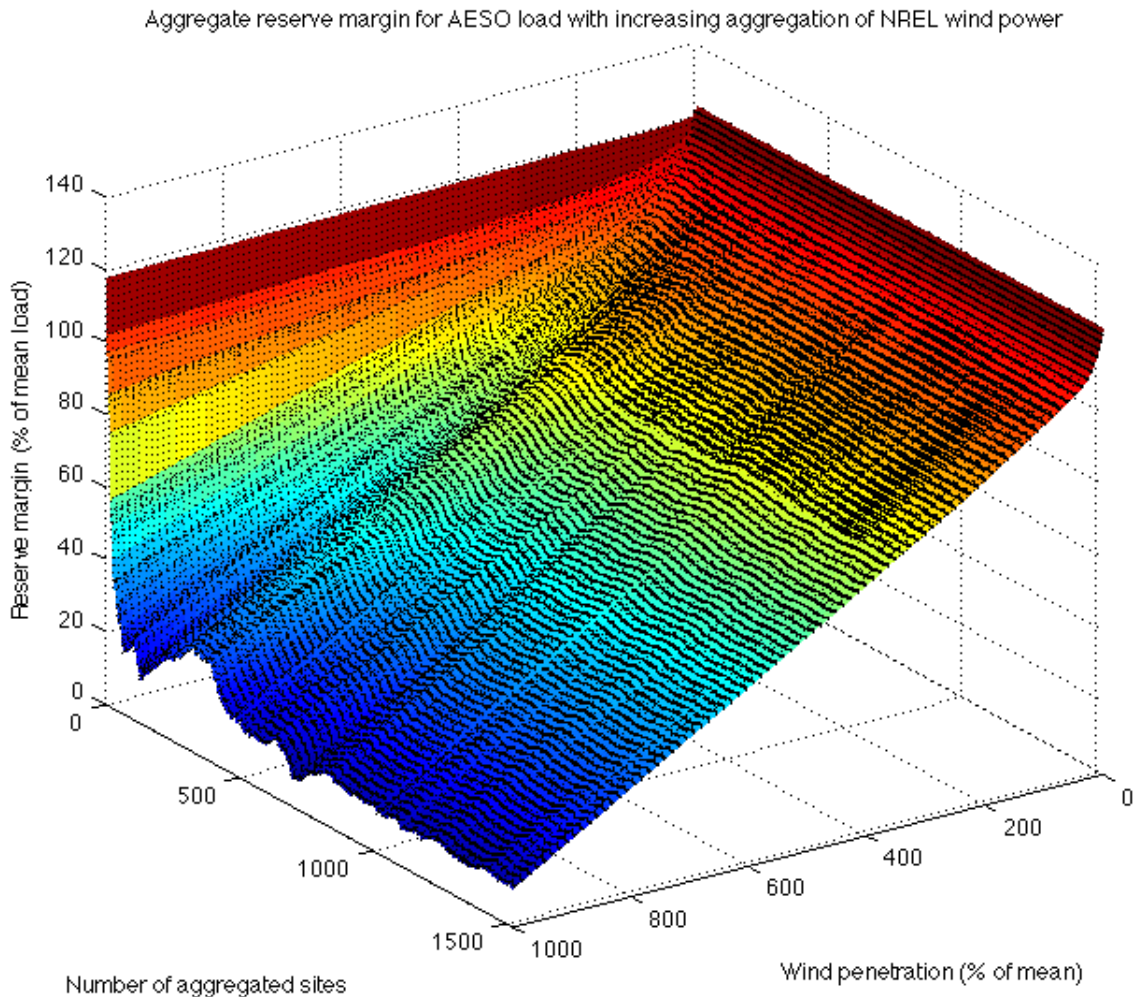


Figure 27. Marginal reserve variation with respect to degree of aggregation and wind penetration

Jointly, the third and fourth hypotheses predict that the reserve margin will be reduced with increasing levels of aggregation. Based on the aggregation level alone, we would expect that the NREL dataset would result in the most reserve margin reduction, followed by the MISO dataset, followed by AESO, followed by the Haina wind farm dataset. However, as is shown in Figure 25, the Haina wind farm dataset actually outperformed the AESO wind power dataset. To further understand the effects of aggregation, the reserve margin calculations for the AESO load were re-calculated for varying levels of aggregation of the NREL wind power dataset. Figure 27 shows that aggregation does have an effect on reserve margin reduction, but exhibits relatively little

reserve margin reduction beyond around 100 wind sites. Thus, hypothesis four is verified, but with the qualification that the degree of aggregation is small. In the sequel, it will be shown that the differences in reserve margin requirements for the AESO, MISO, and Haina wind power datasets are due largely to their correlations with the different load datasets.

It is interesting to note that reserve margin reduction profiles vary widely at low degrees of aggregation. This is illustrated by the probability map of Figure 28 which was formed by running the reserve margin calculations for the AESO load dataset on each individual wind farm location in the NREL dataset. The color spectrum has been scaled logarithmically to highlight the variations at low probability. From Figure 25, it can be noted that the Haina wind dataset is indeed a good representative of a “worst case” wind scenario since the reserve margin for the worst-performing NREL datasets also leveled off around 120% of mean load.

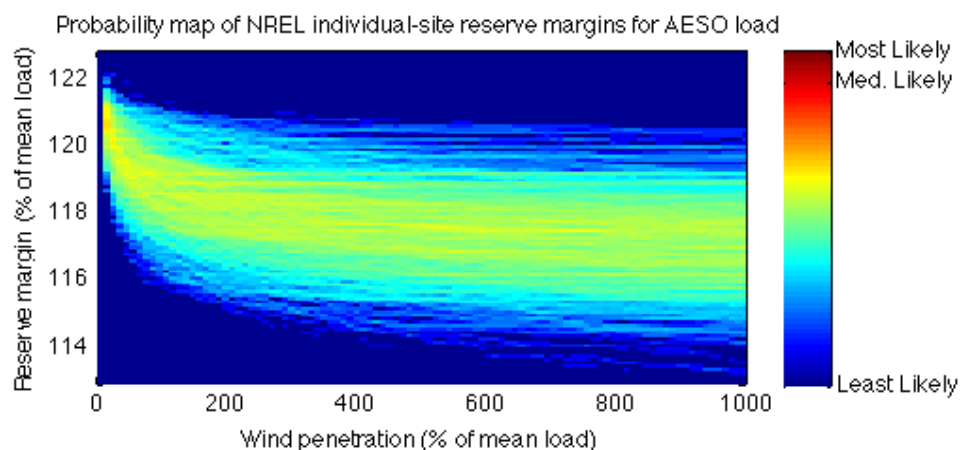


Figure 28. Histograms of marginal reserve requirements for individual sites of the NREL dataset

Auto- and Cross-Correlations

Recall that hypothesis three states that that high correlation of wind power with load has a negative impact on reserve margin reduction. If this is true, we should be able

to order the wind datasets from “best” to “worst” reserve margin reduction performance according to their cross correlation with the load dataset. The correlation information in Figure 29, **Error! Reference source not found.**, and Table 12 produces the set of orderings shown in Table 10 and Table 11. As is shown, the performance ordering obtained by the absolute sum of cross correlation is largely similar to the observed ordering. The incorrect ranking of the Haina wind dataset is likely due to the fact that the Haina dataset produces zero power output for a significant number of samples, while the percentage of “dead time” in the other wind power datasets is negligible.

	Predicted Rank			Observed Rank
	NG Load	MISO Load	AESO Load	
NREL wind	2	1	2	1
MISO wind	3	3	3	2
Haina wind	1	2	1	3
AESO wind	4	4	4	4

Table 10. Reserve margin reduction performance ordering of real wind power

	Predicted Rank			Observed Rank
	NG Load	MISO Load	AESO Load	
Sandia wind	1	1	1	1
SRF wind	3	3	3	2
Weibull wind	2	2	2	3
FG wind	4	4	4	4

Table 11. Reserve margin reduction performance ordering of simulated wind power

	ng load	miso load	aeso load
Haina	15.00	18.10	5.99
miso	137.42	86.59	49.74
aeso	212.84	86.90	69.24
nrel	26.72	16.70	10.18
fg	11.49	12.40	6.01
sandia	0.05	0.05	0.03
srf	0.85	1.04	0.45
wbl	0.74	1.01	0.43

Table 12. Absolute sums of cross correlation functions (from Figure 29 and Error! Reference source not found.)

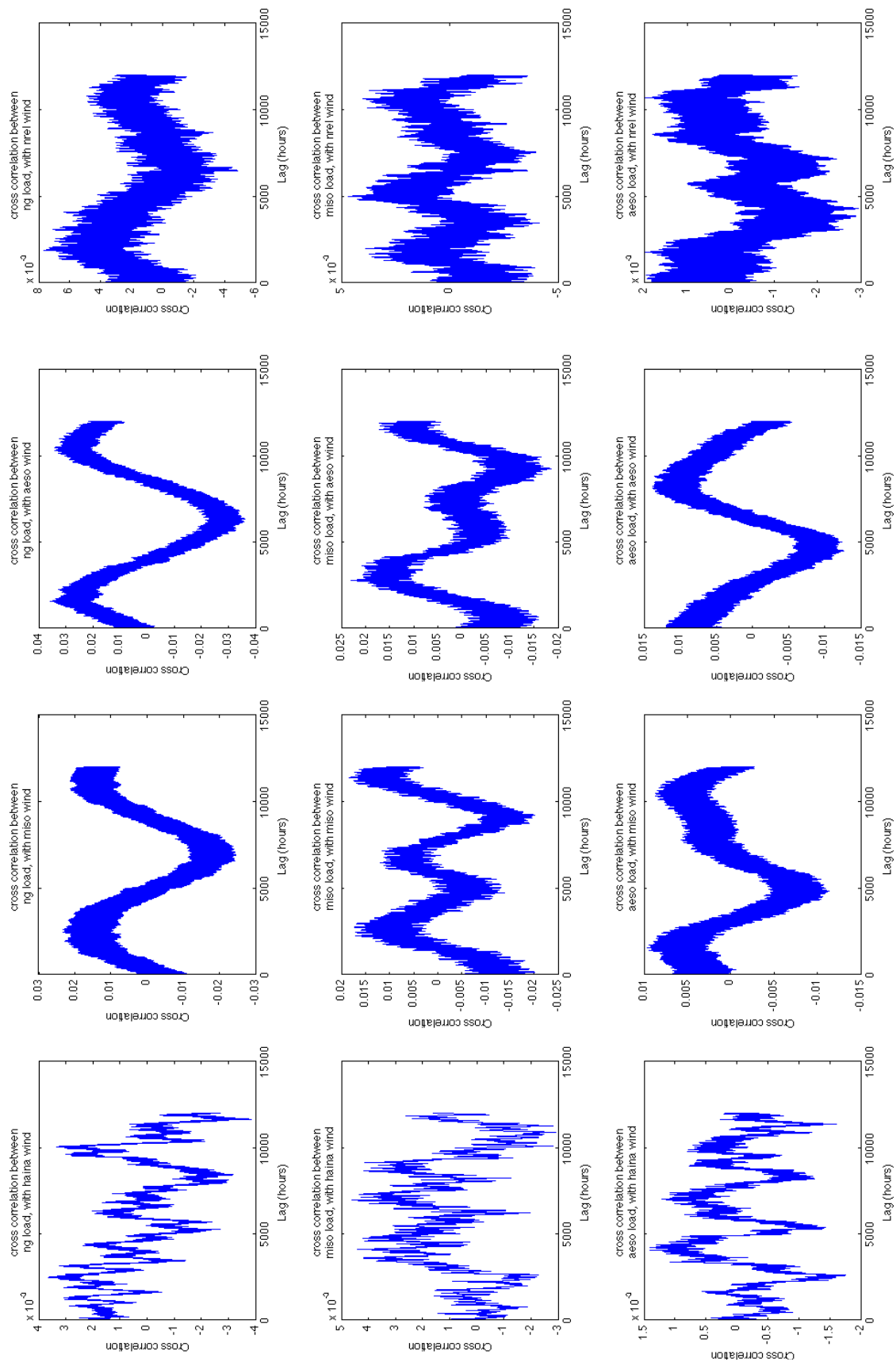


Figure 29. Cross correlations of real-world wind power with the various loads

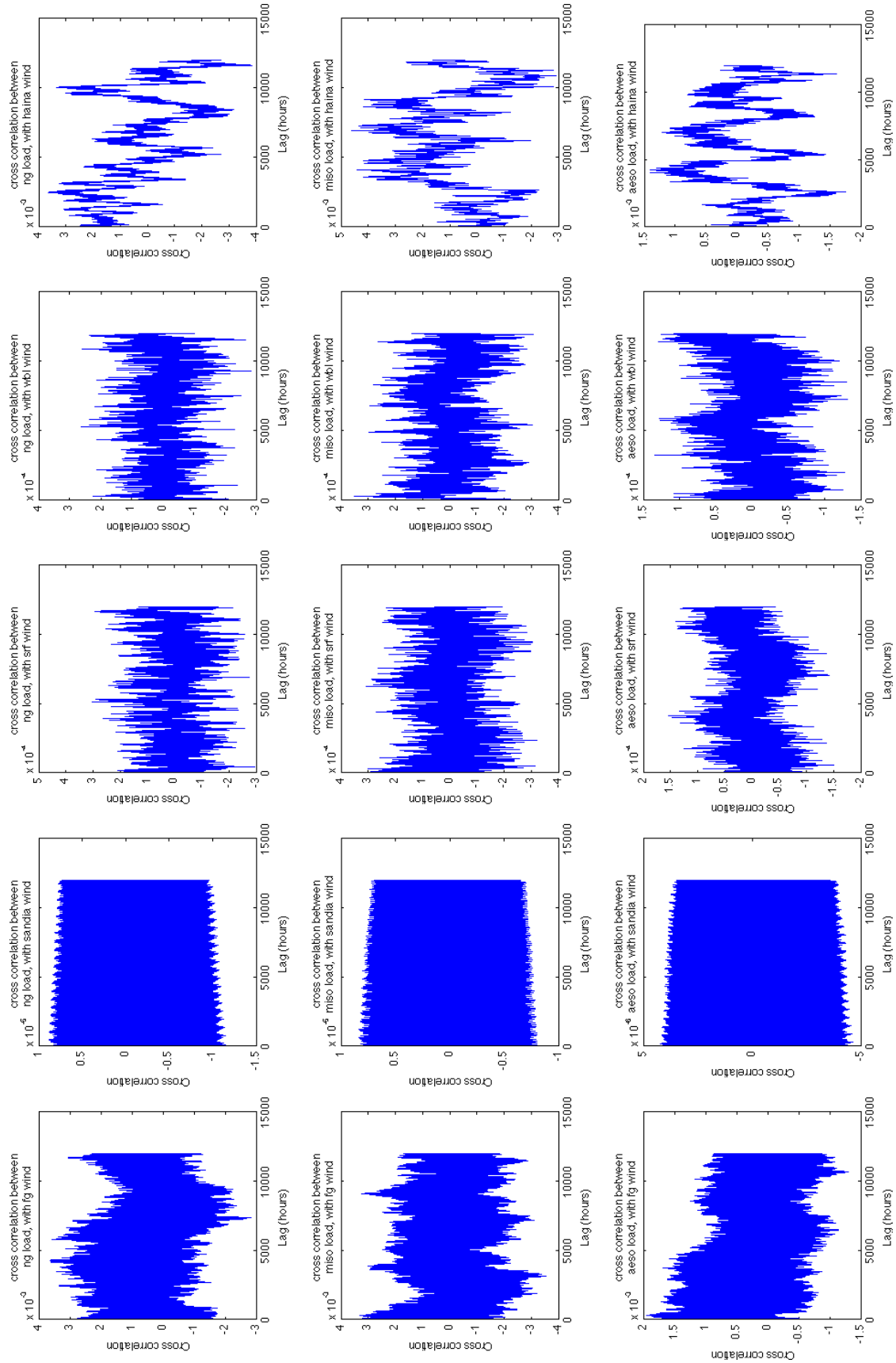


Figure 30. Cross-correlations of simulated wind power with the various loads

While cross-correlation of wind power with load does play an important role in the determination of the reserve margin reduction profile, the autocorrelation of the load or wind does not appear to be a significant predictor of reserve margin performance. This is demonstrated by the results of Table 13 and Table 14, which were computed from Figure 31 and Figure 32.

	Autocorrelation absolute sum	Predicted Rank	Observed Rank
ng	3126.59	2	1
miso	2552.36	1	2
aeso	3469.91	3	3

Table 13. Predicted performance rank of load based on autocorrelation compared to observed rank

	Autocorrelation absolute sum	Predicted Rank	Observed Rank
Haina	613.01	1	3
miso	766.83	3	2
aeso	723.21	2	4
nrel	959.61	4	1

Table 14. Predicted performance rank of real wind power based on autocorrelation compared to observed rank

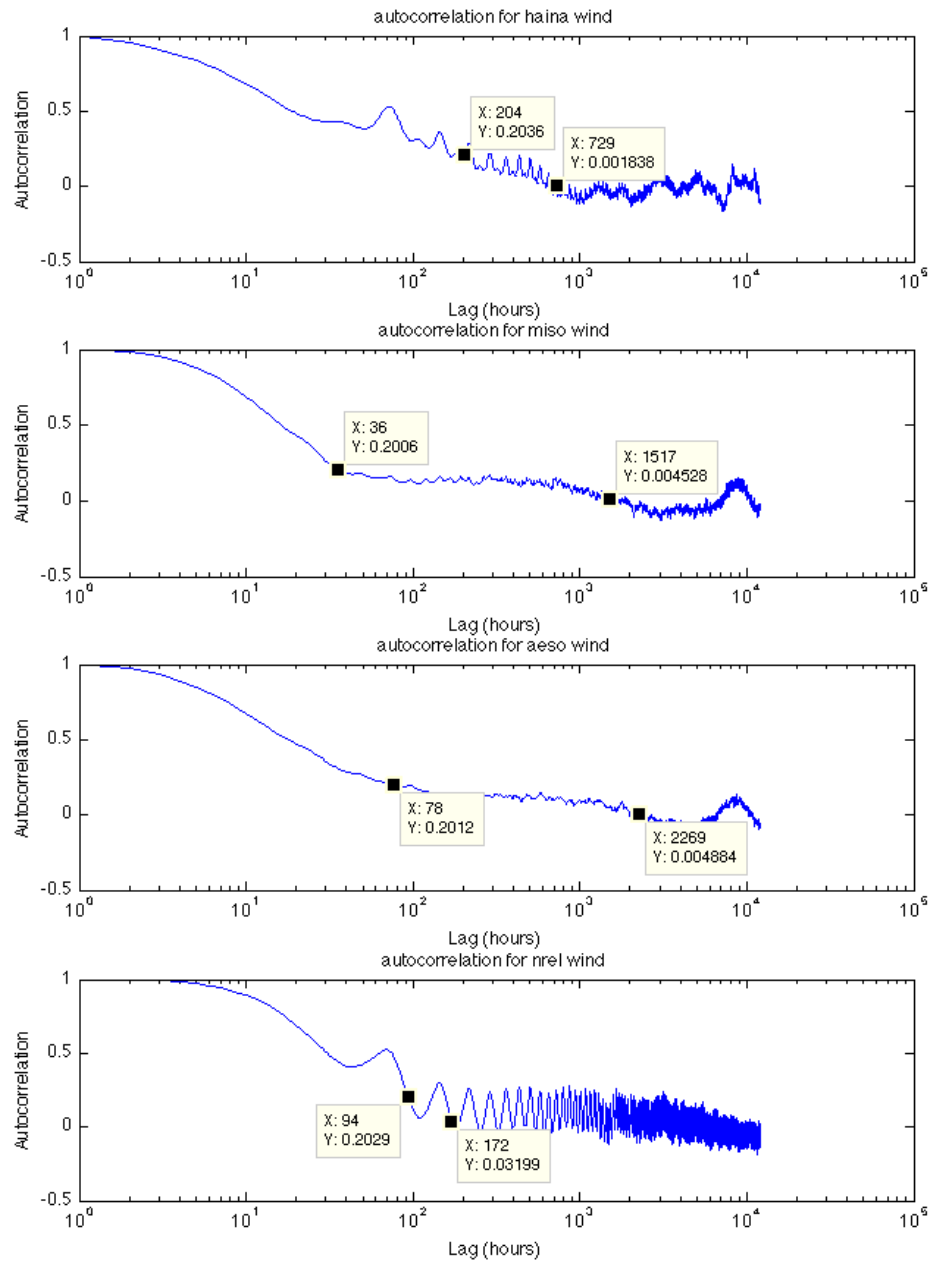


Figure 31. Wind power autocorrelation plots, detailing the lags at which the autocorrelation reaches 20% and 0% of maximum.

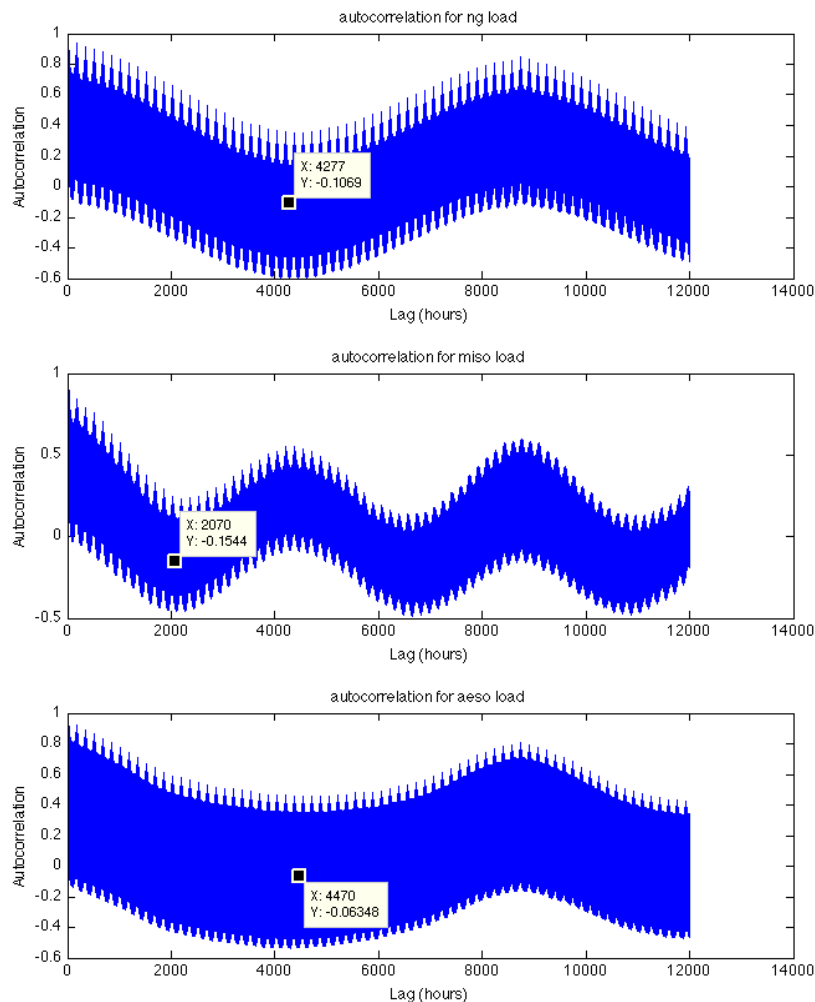


Figure 32. Autocorrelation of loads, detailing location of first large correlation trough.

Effects of energy storage and demand response on RMA

The fifth hypothesis makes the claim that neither energy storage nor demand response have a significant effect at low deployment. This is motivated by the assumption that the spectral power at high frequencies is relatively small compared to the low frequency components of the wind power signal. The power spectra of the loads and wind datasets are shown in Figure 33 and Figure 34, and justify this assumption. The simulated wind power spectrum is shown in Figure 35 for completeness, but this thesis does not consider the effect of energy storage or demand response on the simulated wind power reserve margin reduction.

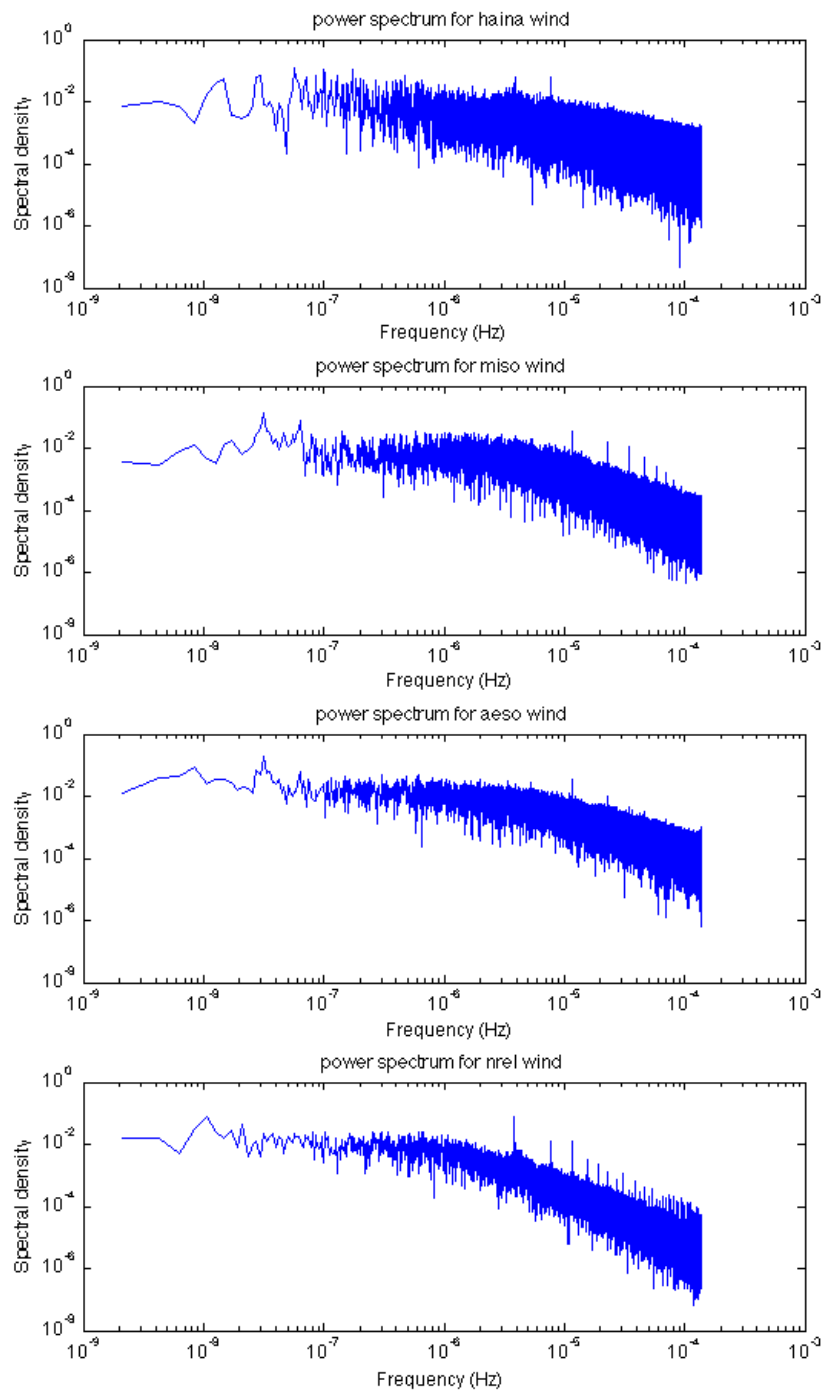


Figure 33. Power spectra of real wind

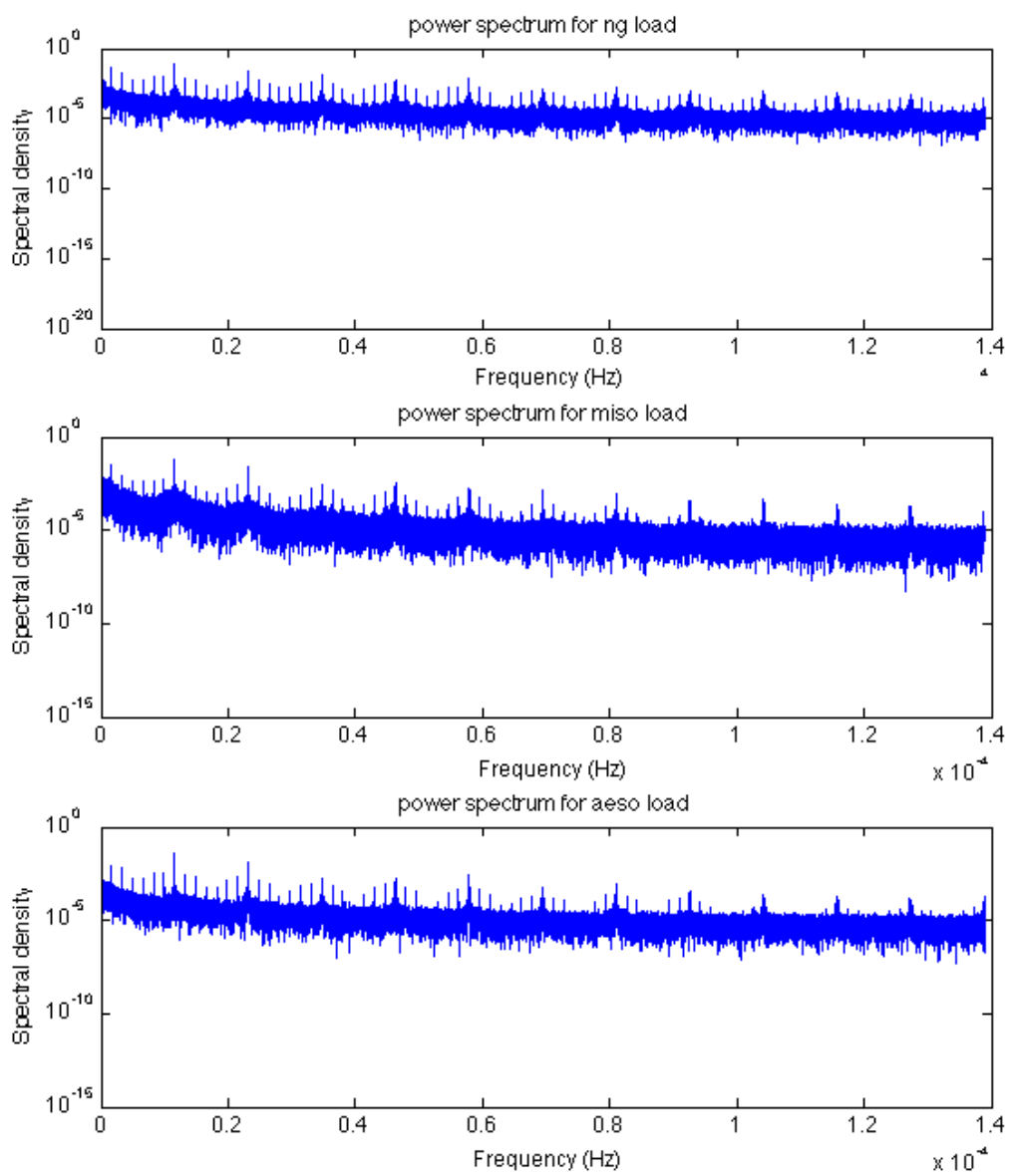


Figure 34. Power Spectra of loads

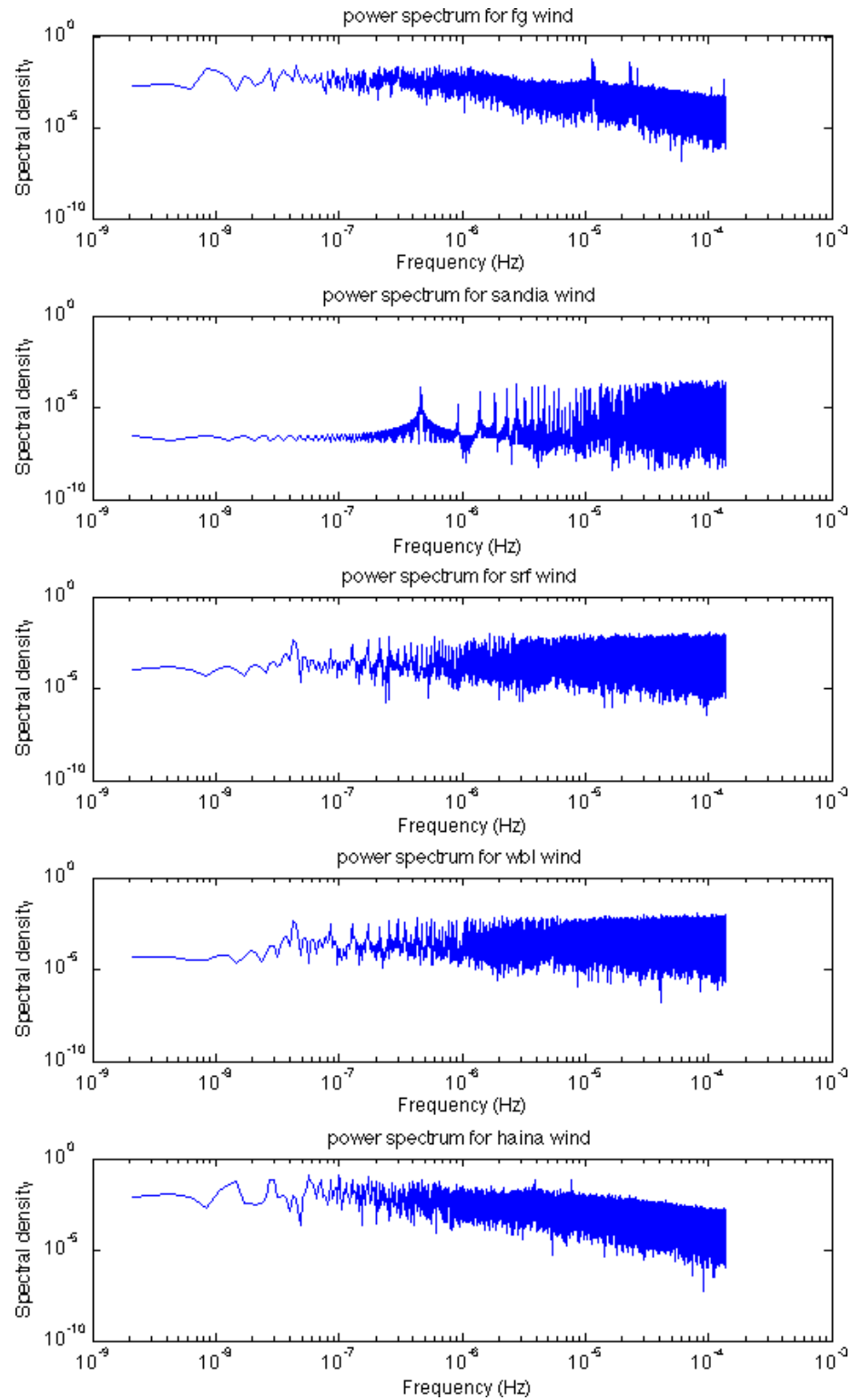


Figure 35. Power spectra of simulated wind

Demand Response

Figure 36, Figure 37, and Figure 38 show the reduction in reserve margin from the case with no demand response at mid term, long term, and extreme case maximum duration ranges respectively. In accordance with hypothesis five, the demand response does not begin to have a significant impact until around 200 hours, corresponding to 1.4×10^{-6} Hz, which is approximately where the spectral densities of the wind power begin to become large. It is also interesting to note that there is very little reserve margin reduction in the low wind penetration situations.

Energy Storage

Figure 39, Figure 40, and Figure 41 show the reduction in reserve margin from the no-storage case at mid, large, and extreme case energy storage capacity respectively. The energy storage simulations showed significantly more variation than the demand response simulations. However, like the demand response simulations, energy storage did not begin to significantly impact reserve margin until it reached a capacity capable of mitigating long-term fluctuations. Surprisingly, energy storage tended to require around an order of magnitude more capacity (in terms of hours of mean wind) than the “virtual storage” represented by the demand response. Thus, the final hypothesis of near one-to-one correspondence between energy storage capacity and demand response was rejected.

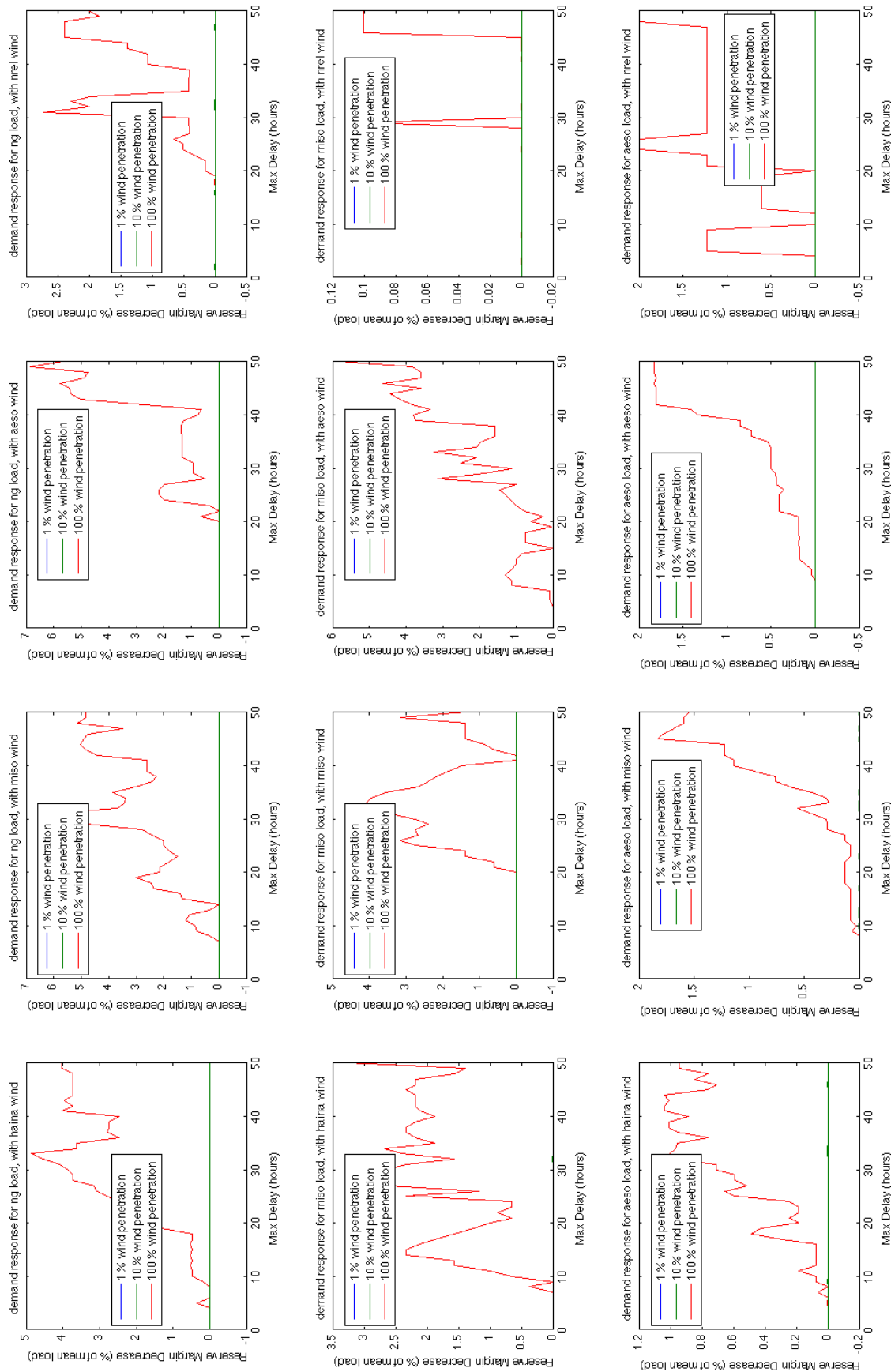


Figure 36. Reserve margin reductions from base-case under “mid term” demand response (up to 50 hours)

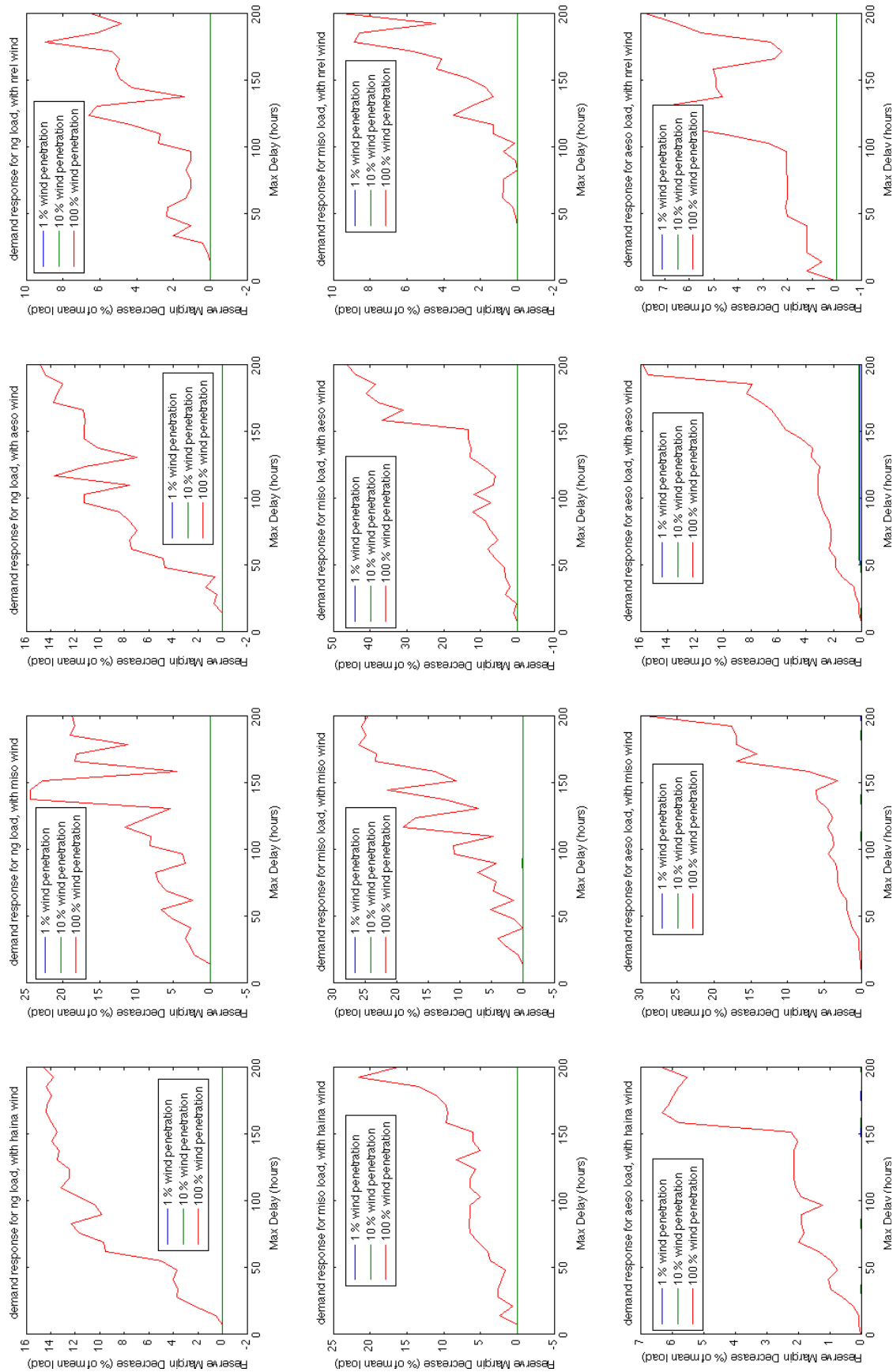


Figure 37. Reserve margin reductions from base-case under “long term” demand response (up to 200 hours)

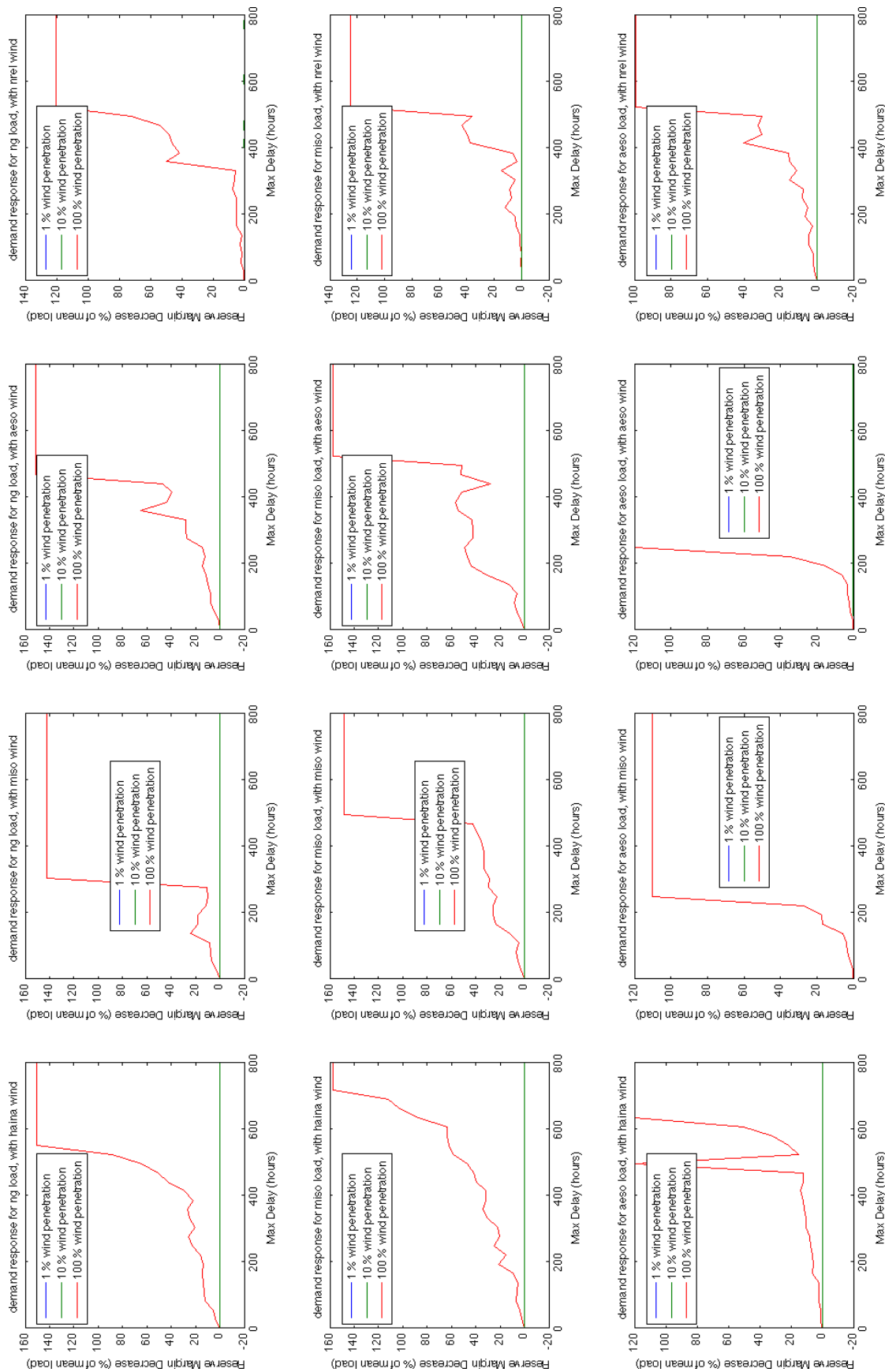


Figure 38. Reserve margin reductions, in extreme case demand response (up to 800 hours)

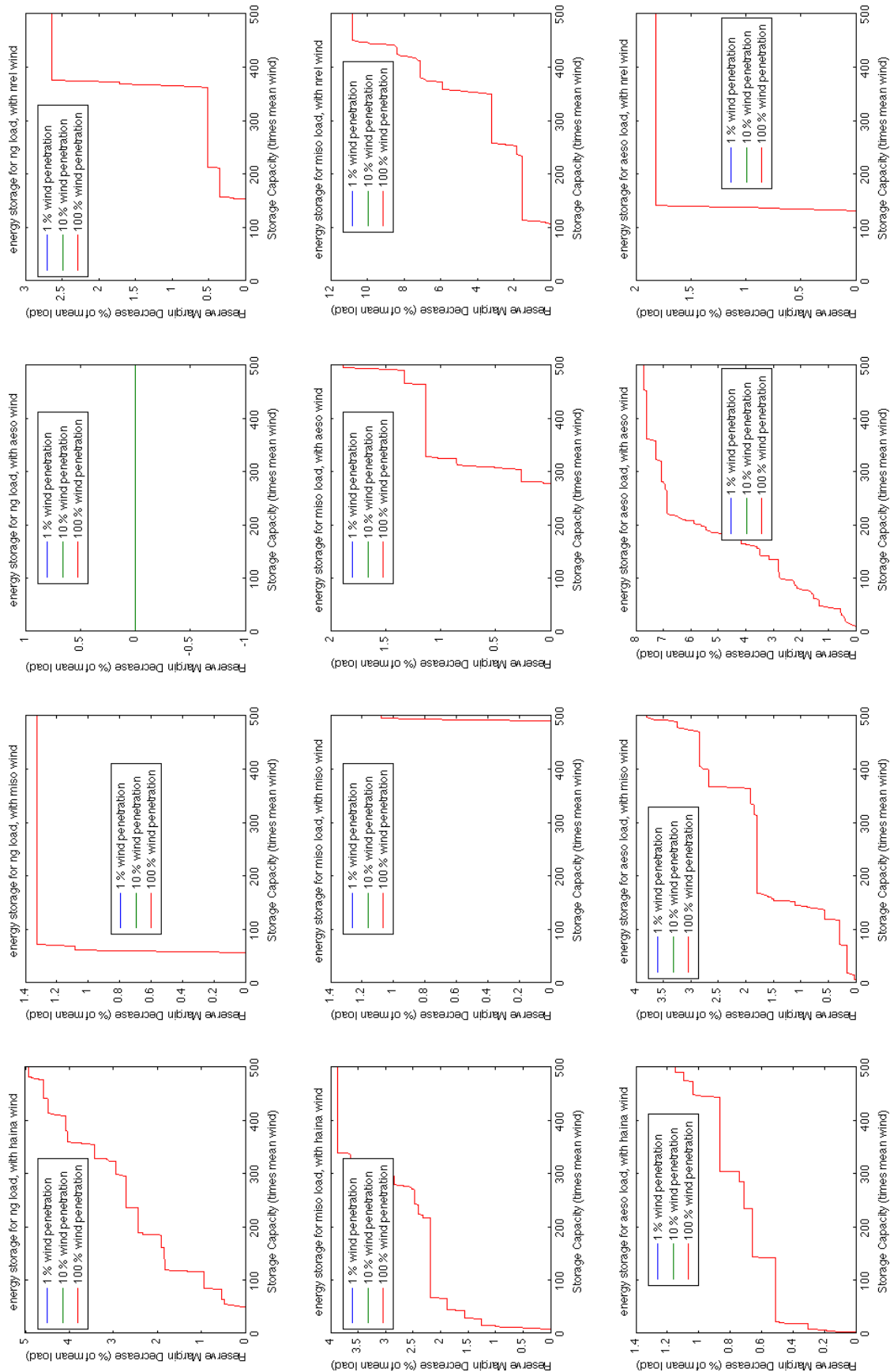


Figure 39. Mid-capacity (up to 500 hours mean wind)

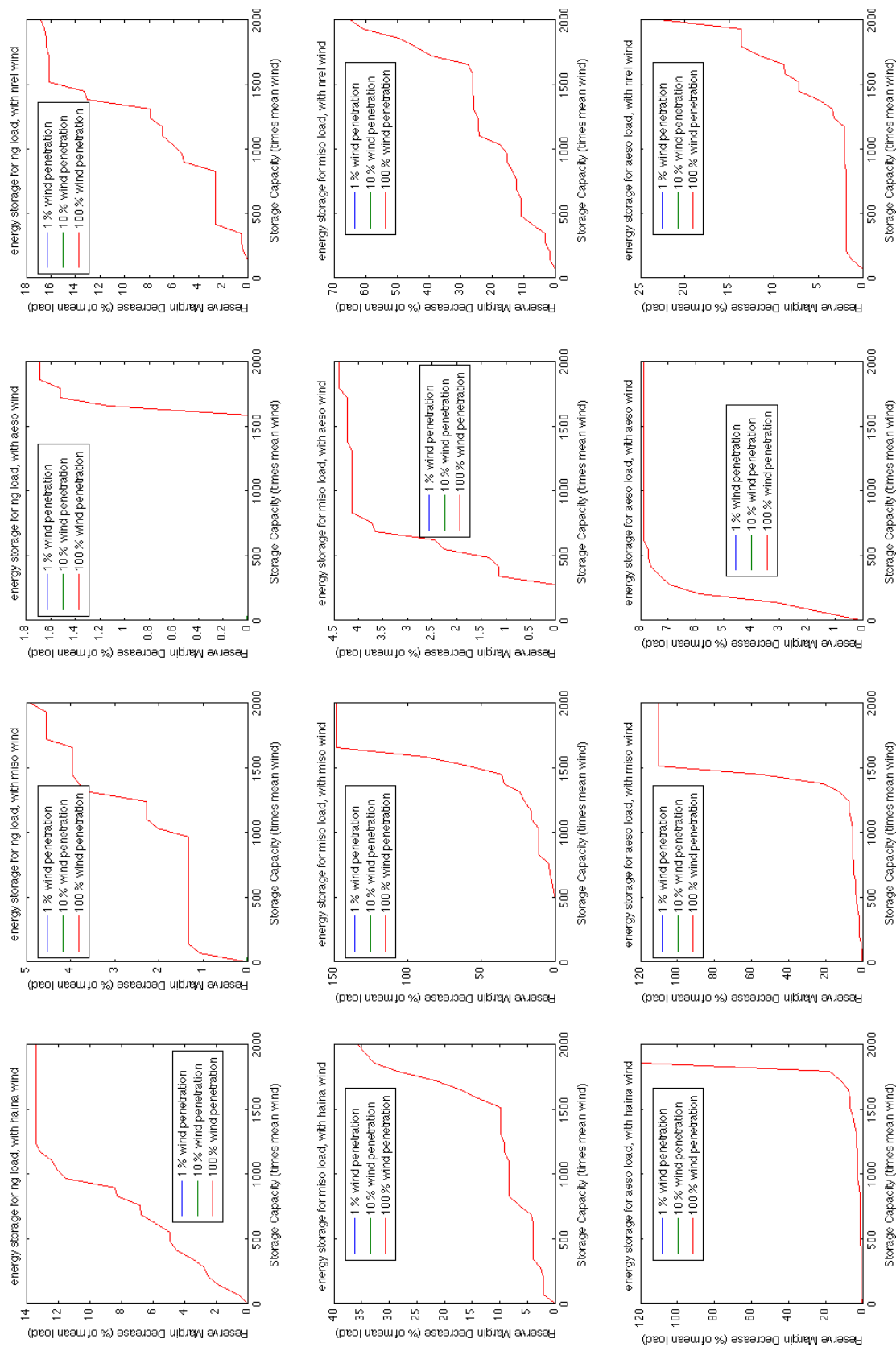


Figure 40. Large capacity (up to 2000 hours of mean wind)

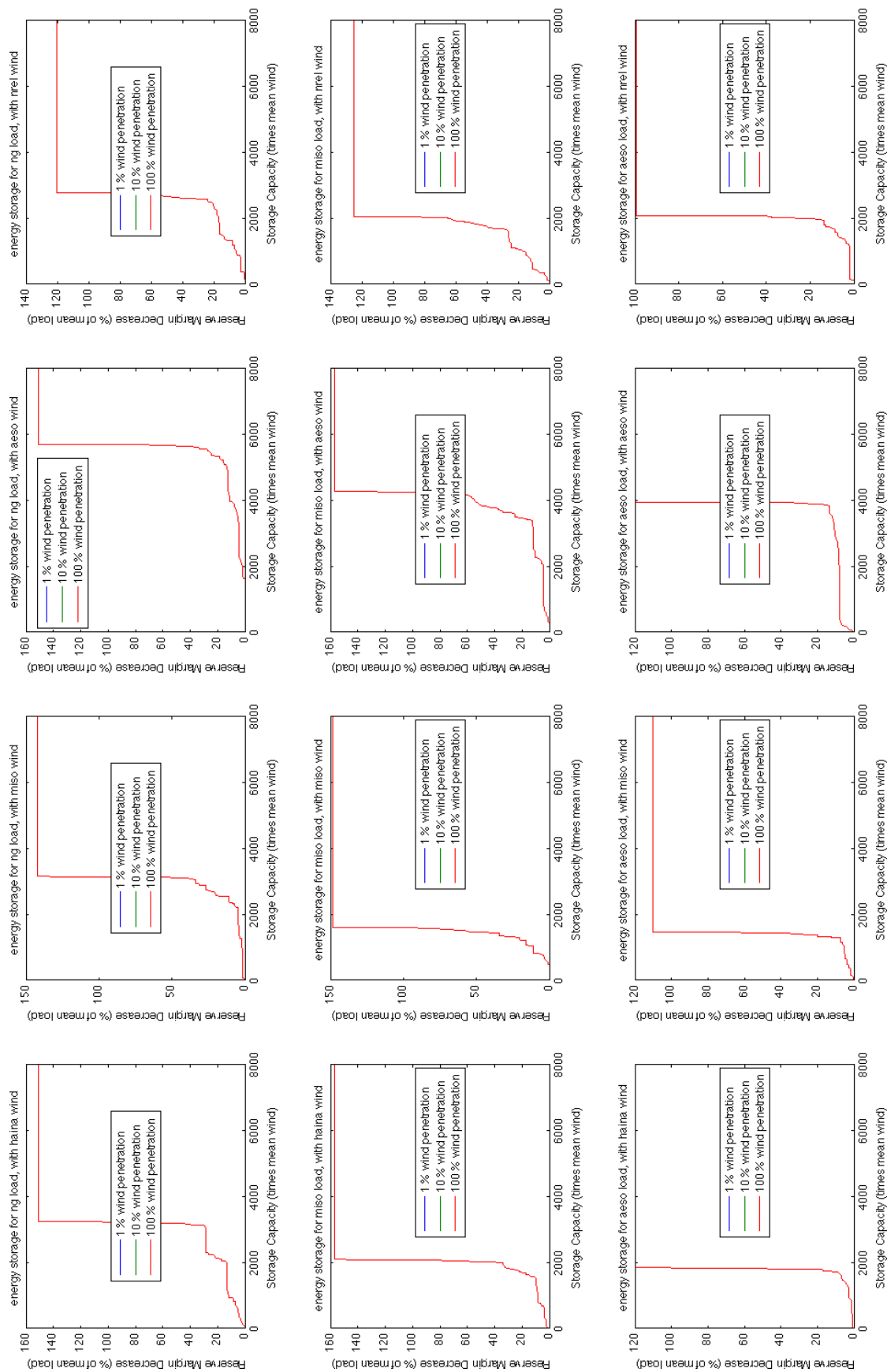


Figure 41. Extreme-case energy storage capacity (up to 8000 hours of mean wind)

CHAPTER 4

CONCLUSION AND FUTURE RESEARCH

It is our hope that the quantitative results of this thesis will spark additional research related to wind energy and the electric grid. This chapter details some particular ways in which our conclusions provide a solid contribution to the wind energy community and offers suggestions on how the research done in this thesis may be extended in the future.

Data Preprocessing and Wind Simulation

In addition to providing detailed descriptions of the steps involved in obtaining useful real-world wind and load data, the preprocessing analysis of this thesis motivates the design of a new wind power model. This model, obtained by filtering of a stationary random variable, is similar to other filtered stationary wind models such as [26], but is unique in that realistic turbulence characteristics are ignored altogether and only the frequency spectrum is considered. Future investigations may compare the behavior of this simplistic model with more physically-motivated models in scenarios related to reserve margin allocation. Moreover, improvements may be made to the filtered Gaussian wind power model so that the long-term probability density characteristics follow a distribution which is more physically realistic.

Reserve Margin Characteristics

Our research verifies that the rate of reserve margin reduction at very low wind penetrations is close to 100% of the additional mean wind. This result indicates that the

wind profile at very low wind penetrations may be treated as statistically independent from the load – for reserve margin calculation purposes. However, as wind penetration increases, the independence assumption quickly becomes invalid and leads to under-allocation of reserve margin. This analysis may be improved in three particular ways.

First, this thesis explicitly evaluates reserve margin allocation with time series datasets. Future research may compare these time series results with a more detailed analysis of long-term statistical descriptions of wind and load profile (such as the cumulative distribution function). This long-term analysis, in turn, may lead to a simpler framework for predicting reserve margin behavior.

Second, our research indicates that cross correlation between wind and load profile is a good indicator of reserve margin reduction performance. To refine these results, a more precise performance metric can be developed that also takes into account some measure of “dead time” in the wind profile. Additionally, more research is needed to determine the precise role that autocorrelation of wind or load profile has on reserve margin reduction behavior.

Third, there are a number of questions related to fundamental reserve margin reduction behavior that remain to be answered. The statistical framework of this thesis may be used in the future to obtain quantitative answers regarding the effects of forecasting and a determination of the optimal wind power curtailment level for minimizing reserve margin. Furthermore, the simulation models may be improved by adding additional practical constraints. For example, ramp-rate restrictions may be added to the reserve generators and/or the energy storage element, and a degree of uncertainty may be added to the demand response model.

Intermittency Mitigation Behavior

This thesis has shown that, contrary to the common intuitive assumption, demand response is decidedly distinct from energy storage in at least one idealized grid

realization. In fact, an effective load shifting type demand response implementation requires about an order of magnitude less “capacity” (in terms of hours of mean wind power) than an ideal energy storage device. The counter-intuitive nature of this result merits a more thorough investigation into the exact relationship between demand response and energy storage. We suggest approaching this investigation from two angles. First, an analysis of the sharp “inflection points” on the reserve margin reduction curves of Figure 38 and Figure 41, as compared to the power spectra of Figure 33 and Figure 34 may explain the differences between energy storage and demand response in terms of frequency characteristics. Second, an inquiry into the effects of asymmetry in the wind power probability distribution as it is related to the increase in required energy storage capacity may explain the differences between energy storage and demand response in terms of long-term statistical characteristics.

Given that residential consumers make up 38% of electricity market [27], it is clear that widespread and effective demand response could have a transformative effect on the electricity industry. In addition to a more accurate articulation of demand response as “virtual storage,” there is also a need for the development and testing of innovative demand response models. The statistical framework of this thesis provides an excellent mechanism for comparing the quantitative effects of these models on reserve margin allocation.

There is a particular need for a “first principles” demand response model which is free from market assumptions and is based directly on the fundamentals of customer behavior. To this end we encourage the development of a non-price-based demand response model, which estimates the effects of behavioral marketing strategies on the energy consumer. The “big picture” motivation for developing a behavioral model for demand response is twofold. First, monetary incentives have been proven to underestimate true customer response potential [28][29]. Second, there is a need to develop sustainable energy marketing strategies that address “value” rather than strict

cost. Not only does [30] show that the majority of consumers are unaware of their own energy usage, but [31] indicates that electricity accounts for less than 3% of household spending. Therefore, even the potential for a 10% decrease in the monthly electric bill may not be “valuable” enough to change customer habits.

BIBLIOGRAPHY

- [1] H. Ibrahim, M. Ghandour, M. Dimitrova, A. Ilinca, and J. Perron, "Integration of Wind Energy into Electricity Systems: Technical Challenges and Actual Solutions," *Energy Procedia*, vol. 6, pp. 815–824, 2011.
- [2] Loss of Load Expectation Working Group and Regulatory and Economic Studies Department, "Planning Year 2012 LOLE Study Report," Midwest Independent System Operator, 2012.
- [3] A. D. Lamont, "Assessing the long-term system value of intermittent electric generation technologies," *Energy Economics*, vol. 30, pp. 1208–1231, May 2008.
- [4] M. Parry, "Climate change: where should our research priorities be?," *Global Environmental Change*, vol. 11, no. 4, pp. 257–260, Dec. 2001.
- [5] L. Soder, "Reserve margin planning in a wind-hydro-thermal power system," *Power Systems, IEEE Transactions on*, vol. 8, no. 2, pp. 564–571, May 1993.
- [6] P. Wang, L. Goel, Y. Ding, L. P. Chang, and M. Andrew, "Reliability-based long term hydro/thermal reserve allocation of power systems with high wind power penetration," in *Power Energy Society General Meeting, 2009. PES '09. IEEE*, 2009, pp. 1–7.
- [7] P. Ahcin and M. Sikic, "Simulating demand response and energy storage in energy distribution systems," in *IEEE International Conference on Power System Technology POWERCON, Hangzhou, China*, 2010.
- [8] T. K. A. Brekken, A. Yokochi, A. von Jouanne, Z. Z. Yen, H. M. Hapke, and D. A. Halamay, "Optimal Energy Storage Sizing and Control for Wind Power Applications," *Sustainable Energy, IEEE Transactions on*, vol. 2, no. 1, pp. 69–77, Jan. 2011.
- [9] M. H. Albadi and E. F. El-Saadany, "A summary of demand response in electricity markets," *Electric Power Systems Research*, vol. 78, no. 11, pp. 1989–1996, Nov. 2008.
- [10] R. Munson, *From Edison to Enron: the business of power and what it means for the future of electricity*. Westport, Conn.: Praeger Publishers, 2005.
- [11] "Milestones:List of IEEE Milestones - GHN: IEEE Global History Network." [Online]. Available: http://www.ieeeighn.org/wiki/index.php/Milestones:List_of_IEEE_Milestones. [Accessed: 26-May-2012].
- [12] J. Jonnes, *Empires of light: Edison, Tesla, Westinghouse, and the race to electrify the world*. New York: Random House, 2003.
- [13] "Global Trends in Renewable Energy Investment 2011 Report."

- [14] J. P. Barton and D. G. Infield, "Energy Storage and Its Use With Intermittent Renewable Energy," *IEEE Transactions on Energy Conversion*, vol. 19, pp. 441–448, Jun. 2004.
- [15] K. Spees and L. B. Lave, "Demand Response and Electricity Market Efficiency," *The Electricity Journal*, vol. 20, no. 3, pp. 69–85, Apr. 2007.
- [16] G. Calabrese, "Determination of Reserve Capacity by the Probability Method," *American Institute of Electrical Engineers, Transactions of the*, vol. 69, no. 2, pp. 1681–1689, Jan. 1950.
- [17] J. Seguro, "Modern estimation of the parameters of the Weibull wind speed distribution for wind energy analysis," *Journal of Wind Engineering and Industrial Aerodynamics*, vol. 85, pp. 75–84, Mar. 2000.
- [18] I. Y. . Lun and J. C. Lam, "A study of Weibull parameters using long-term wind observations," *Renewable Energy*, vol. 20, no. 2, pp. 145–153, Jun. 2000.
- [19] S. Rehman, T. O. Halawani, and T. Husain, "Weibull parameters for wind speed distribution in Saudi Arabia," *Solar Energy*, vol. 53, no. 6, pp. 473–479, Dec. 1994.
- [20] A. N. Kolmogorov, "The Local Structure of Turbulence in Incompressible Viscous Fluid for Very Large Reynolds Numbers," *Proceedings of the Royal Society A: Mathematical, Physical and Engineering Sciences*, vol. 434, no. 1890, pp. 9–13, Jul. 1991.
- [21] J. Apt, "The spectrum of power from wind turbines," *Journal of Power Sources*, vol. 169, no. 2, pp. 369–374, Jun. 2007.
- [22] "Turbine overview. Wind. It means the world to us. | Vestas." [Online]. Available: <http://www.vestas.com/en/wind-power-plants/procurement/turbine-overview.aspx#/vestas-univers>. [Accessed: 18-Jun-2012].
- [23] P. S. Veers, *Three-dimensional wind simulation*. 1988.
- [24] R. G. Lane, A. Glindemann, and J. C. Dainty, "Simulation of a Kolmogorov phase screen," *Waves in Random Media*, vol. 2, no. 3, pp. 209–224, 1992.
- [25] K. Brokish and J. Kirtley, "Pitfalls of modeling wind power using Markov chains," 2009, pp. 1–6.
- [26] C. Nichita, D. Luca, B. Dakyo, and E. Ceanga, "Large band simulation of the wind speed for real time wind turbine simulators," *Energy Conversion, IEEE Transactions on*, vol. 17, no. 4, pp. 523 – 529, Dec. 2002.
- [27] U.S. Energy Information Administration, "Annual Energy Review 2010," Office of Energy Statistics, U.S. Department of Energy.
- [28] W. Abrahamse, L. Steg, C. Vlek, and T. Rothengatter, "A review of intervention studies aimed at household energy conservation," *Journal of Environmental Psychology*, vol. 25, no. 3, pp. 273–291, Sep. 2005.
- [29] S. J. Kantola, G. J. Syme, and N. A. Campbell, "Cognitive dissonance and energy conservation.," *Journal of Applied Psychology*, vol. 69, no. 3, pp. 416–421, 1984.

- [30] S. Z. Attari, M. L. DeKay, C. I. Davidson, and W. B. D. Bruin, “Public Perceptions of Energy Consumption and Savings,” *PNAS*, vol. 107, no. 37, pp. 16054–16059, Sep. 2010.
- [31] “Consumer Expenditure Survey.” [Online]. Available: <http://www.bls.gov/cex/>. [Accessed: 18-Jun-2012].